Ground-Water Flow and Migration of Hydrocarbons to the Lower Permian White Rim Sandstone, Tar Sand Triangle, Southeastern Utah

U.S. GEOLOGICAL SURVEY BULLETIN 2000–J

Cover. View south toward the LaSal Mountains along the Colorado River between Cisco and Moab, Utah. Fisher Towers in center is composed of Permian Cutler Formation and capped by Triassic Moenkopi Formation. The prominent mesa at left center is capped by Jurassic Kayenta Formation and Wingate Sandstone and underlain by slope-forming Triassic Chinle and Moenkopi Formations. The Chinle-Moenkopi contact is marked by a thin white ledge-forming gritstone. The valley between Fisher Towers and Fisher Mesa in the background is part of Richardson Mesa, part of Professor Valley. Photograph by Omer B. Raup, U.S. Geological Survey.

Ground-Water Flow and Migration of Hydrocarbons to the Lower Permian White Rim Sandstone, Tar Sand Triangle, Southeastern Utah

By Richard F. Sanford

EVOLUTION OF SEDIMENTARY BASINS—PARADOX BASIN
A.C. Huffman, Jr., Project Coordinator

U.S. GEOLOGICAL SURVEY BULLETIN 2000–J

A multidisciplinary approach to research studies of sedimentary rocks and their constituents and the evolution of sedimentary basins, both ancient and modern

UNITED STATES GOVERNMENT PRINTING OFFICE, WASHINGTON : 1995

U.S. DEPARTMENT OF THE INTERIOR
BRUCE BABBITT, Secretary

U.S. GEOLOGICAL SURVEY
Gordon P. Eaton, Director

For sale by U.S. Geological Survey, Information Services
Box 25286, Federal Center
Denver, CO 80225

Library of Congress Cataloging-in-Publication Data

Sanford, Richard F.
Ground-water flow and migration of hydrocarbons to the Lower Permian White Rim Sandstone, Tar Sand Triangle, southeastern Utah / by Richard F. Sanford.
p. cm. — (Evolution of sedimentary basins—Paradox Basin ; J) (U.S. Geological Survey bulletin ; 2000)
Includes bibliographical references (p. -)
Supt. of Docs. no.: I 19.2:B2000J
1. Groundwater flow—Utah. 2. Petroleum—Migration—Utah. 3. White Rim Sandstone (Utah) I. Title. II. Series. III. Series: U.S. Geological Survey bulletin ; 2000.
QE75.B9 no. 2000-J
[GB1197.7]
557.3 s—dc20
[553.2'8'09792 95-11114
CIP

CONTENTS

FIGURES

TABLES

Ground-Water Flow and Migration of Hydrocarbons to the Lower Permian White Rim Sandstone, Tar Sand Triangle, Southeastern Utah

By Richard F. Sanford[1]

ABSTRACT

The Lower Permian White Rim Sandstone in the Tar Sand Triangle of southeastern Utah contains an estimated 12.5–16 billion barrels of heavy oil. Despite the large size of the deposit, the source of its oil is unknown. This paper systematically discusses source rocks for this petroleum from the standpoint of hydrocarbon abundance and maturity and ground-water flow history. Ground-water flow through the White Rim Sandstone was governed by six periods, each characterized by distinct paleotopographic conditions and directions of horizontal flow. Analysis of the transmissivity and thickness of the hydrostratigraphic units indicates that flow was mainly horizontal and had no major vertical component. Long-range transport of petroleum through Pennsylvanian and Permian sandstone aquifers that were hydrologically continuous with the White Rim was possible until Late Cretaceous to Paleocene Sevier thrusting. After thrusting, long-range migration would have been impeded or diverted by the thrust faults. Ten potential source-rock units are identified in the area. Some are unfavorable because they lack sufficient organic matter to account for the hydrocarbons in the Tar Sand Triangle. Others, particularly those in northern Utah, are unfavorable because ground water never flowed in the required direction. Sources to the southwest and southeast are hydrologically favorable. The Paradox Formation of the Hermosa Group is hydrologically favorable, but the pattern of bleaching of the Cutler Group redbeds and the eastward thinning of the White Rim are unfavorable. The Chainman Shale and other formations in Nevada are consistent with east- and northeast-flowing ground water, but migration across the thrust belt is problematic. The most likely source is the Late Proterozoic Chuar Group in west-central Utah. It is compatible with eastward and northeastward ground-water flow, with bleaching of the Permian aquifers, and with continuous sandstone aquifers east of the thrust belt, and it probably has sufficient mature organic matter to account for the oil in the Tar Sand Triangle.

[1]U.S. Geological Survey, MS 905, Denver, Colorado 80225.

INTRODUCTION

The Tar Sand Triangle in the Canyonlands area of southeastern Utah contains the largest accumulation of heavy oil ("tar") in the United States (Demaison, 1977). Most of the oil is in the Lower Permian White Rim Sandstone of the Cutler Group, but a small portion is in the Cedar Mesa Sandstone of the Cutler Group (Campbell and Ritzma, 1979). Heavy oil in place is estimated at 12.5–16 billion barrels (Campbell and Ritzma, 1979). The White Rim consists of sandstone erg deposits modified by coastal marine processes (Steele, 1987; Chan and Kocurek, 1988; Chan, 1989). The tar is in a classic stratigraphic trap formed by pinchout to the southeast of the White Rim Sandstone against the Monument uplift (Baars and Seager, 1970). Oil is concentrated in zones of particularly thick sandstone that have been variously interpreted as offshore marine bars (Baars and Seager, 1970) and as eolian dunes modified by marine processes (Huntoon and Chan, 1987; Tubbs, 1989). Proposed sources for the oil include the Lower Permian Kaibab Formation and the Lower Triassic Sinbad Limestone Member of the Moenkopi Formation (Baars and Seager, 1970) and the Lower Permian Phosphoria Formation (Demaison, 1977). No study to date has systematically surveyed and evaluated all the possible hydrocarbon source rocks, and no study has considered petroleum migration in terms of paleohydrologic evolution.

This paper systematically examines petroleum source rocks from the standpoint of hydrocarbon abundance and maturity and ground-water flow history. Ground-water flow history is reconstructed from paleoenvironmental data, and periods of similar ground-water flow directions are identified. Transmissivities of the hydrostratigraphic units in the Canyonlands area are examined to identify local vertical flow directions. Pennsylvanian and Permian aquifers in Utah and adjacent States are identified to determine the feasibility of long-distance horizontal transport. Potential hydrocarbon source rocks are described with particular attention to quantity, maturation level, and timing of maturation. The bleaching of rocks in the Canyonlands area is used to indicate the flow of organic-acid-bearing ground water. Finally, all these

factors are integrated to select a preferred hydrocarbon source rock.

It is assumed that paleo-ground-water flow was in the direction of paleo-surface-water flow. This is a good approximation for modern systems. Anisotropy of hydraulic conductivity potentially would make ground-water flow deviate from surface-water flow, but generally this effect is small, and data to compute this effect in the Colorado Plateau are unavailable. In addition, it is assumed that oil migrated in the direction of paleo-ground-water flow in the horizontal plane. Both oil and water are subject to the same pressure field, so horizontal flow directions should be similar; however, the *rate* of flow may vary because of the different viscosities, and, in the vertical direction, buoyancy causes oil to rise relative to water (Hubbert, 1953). Despite the expected differences in flow rate and vertical flow direction, the horizontal flow direction is the main constraint for identification of oil source rocks for the Tar Sand Triangle, and it should be predictable from the horizontal ground-water flow directions.

Acknowledgments.—Discussions with Tony Bryant, Paula Hansley, Jackie Huntoon, Art Geldon, Ben Law, Vito Nuccio, and Jim Palacas improved this paper, which was reviewed by Vito Nuccio and Jim Palacas.

PALEOTOPOGRAPHIC HISTORY

The critical control on ground-water flow in a mature uplifted basin is topographic slope (Kreitler, 1989; Garven and others, 1993). Topographic slope provides the major driving force for large-scale regional ground-water flow. This study assumes that ground-water flow parallels the regional topographic gradient. The direction of ground-water flow is inferred from sediment current directions, provenance of source materials, and location of known uplifts.

Ground-water flow through the White Rim Sandstone was governed by six periods, each characterized by distinct paleotopographic conditions (table 1).

1. From the end of Late Permian White Rim deposition (256 Ma) to the end of the Middle to Late Jurassic J5 unconformity (155 Ma) was a long period of time (99 m.y.) during which gradients were low and topographic slopes, and thus ground-water flow, were dominantly northwestward, locally southwestward, and rarely eastward. Local ground-water flow was important, particularly processes such as mixing of sea water with discharging ground water, evaporation in coastal sabkhas, and evaporative pumping that typify low-gradient coastal zones in arid environments. The low slopes and arid environment would have resulted in limited regional ground-water flow. Deposition and compaction during this period was slow. The mean deposition rate was a maximum of 0.011 mm/yr (37 ft/m.y.) for the entire period including major unconformities but averaged 0.03–0.09 mm/yr (100–300 ft/m.y.) during depositional periods. Ground water consisted of trapped sea water, hypersaline brine, and, locally, fresh water.

The Permian-Triassic unconformity at the top of the White Rim Sandstone is marked by conglomerate-filled channels that indicate a western source (Huntoon, 1992). Thus, the first ground water in the White Rim flowed eastward during at least part of the time of the unconformity. The dominant direction of flow, however, was westward off the Uncompahgre uplift. Some of the marine pore water in the White Rim Sandstone may have been flushed out by fresh water at this time.

The Lower and Middle(?) Triassic Moenkopi Formation was deposited on an almost flat coastal plain of a sea that encroached from the northwest (fig. 1) (Stewart and others, 1972; Ochs and Chan, 1990; Blakey and others, 1993). Sea-level changes, sediment supply, and climatic changes led to four transgressive-regressive cycles (Blakey and others, 1993). Numerous depositional environments are recognized from offshore marine to alluvial fan, but the dominant environments are nearshore marine. Ground water flowed dominantly northwestward toward the sea, but southwestward flow off the Uncompahgre uplift was important in the eastern part of the area. Fluvial environments would have favored recharge of fresh ground water. An unconformity marks a period of erosion between the Moenkopi and Upper Triassic Chinle Formations. Because both formations are dominated by a northwest slope, flow during the erosional period probably also was northwest.

The Chinle Formation consists of fluvial and lacustrine clastic sediments deposited in six depositional cycles (Stewart and others, 1972; Blakey and Gubitosa, 1983). Inferred ground-water flow was dominantly to the northwest but included tributary southwestward flow off the Uncompahgre uplift (fig. 2). The fluvial environments suggest higher slope than that of the Moenkopi. Paleoclimate reconstruction suggests a monsoonal climate (Dubiel and others, 1991), and thus major seasonal recharge of fresh ground water.

The Lower Jurassic Glen Canyon Group is composed of eolian and fluvial sediments. The eolian Wingate Sandstone unconformably overlies the Chinle. Erg-margin deposits southwest of the Canyonlands area indicate continuation of the dominant northwestward gradient (fig. 3) (Clemmensen and others, 1989). The gradient in the Canyonlands area may have been southwestward, similar to the gradient of the overlying Kayenta Formation. The fluvial Kayenta Formation indicates a westward flow direction (fig. 4) (Molenaar, 1971; Peterson, 1988) that is probably due to rejuvenation of the Uncompahgre uplift. Recharge of fresh ground water would have taken place during Kayenta deposition. The eolian Navajo Sandstone represents a major sand sea. Ground-water flow directions are unknown, but continuation of previous trends would suggest northwest and southwest flow directions.

The Middle Jurassic San Rafael Group is composed of dominantly marine clastic sediments and lesser eolian

Table 1. Stratigraphic and paleohydrologic data on Post-White Rim Sandstone units.

[Data from Baars and Molenaar (1971), Clemmensen and others (1989), Cobban and Hook (1989), Craig (1981), Dubiel (1994), Fouch and others (1983), Franczyk and others (1990), Freethey and Cordy (1991), Geldon (in press), Gill and Hail (1975), Hansen (1991), Harland and others (1990), Imlay (1980), Kowallis and Heaton (1987), Kowallis and others (1991), Molenaar and Baars (1985), Obradovich (in press), Padian (1989), Peterson (1994), Willis and Kowallis (1988), and Wing and others (1991)]

Period	Series or stage	Group	Formation, event, or feature	Thickness (feet) From	Thickness (feet) To	Age at start (Ma)	Deposition rate (ft/yr) From	Deposition rate (ft/yr) To	Direction	Slope	Period
TERTIARY-QUATERNARY											
Late Miocene-Holocene		Grand Canyon cutting				10.0	0	0	Southwest	High	6
TERTIARY											
Late Eocene–early Miocene		Unconformity				40.0		0 ?		Low	5
Early-middle Eocene		Wasatch Formation		1,800	1,800	56.0	113	113	Northwest	Med	5
Paleocene		Unconformity				65.4	0	0	North?	Low	5
CRETACEOUS											
Maastrichtian		Unconformity				71.3	0	0	North?	Low	5
Middle late Campanian–Maastrichtian	Mesaverde	Farrer Formation-Tuscher Formation		1,000	1,000	74.0	370	370	Northeast-north	Medium	5
Middle late Campanian	Mesaverde	Neslen Formation–Mount Garfield Formation		600	600	76.0	300	300	East	Medium	4
Late Campanian	Mesaverde	Sego Sandstone		50	200	76.6	83	333	East	Low	4
Late Campanian	Mesaverde	Mancos Shale (Buck Tongue)		0	200	78.5	0	105	--	0	3
Early late Campanian	Mesaverde	Castlegate Sandstone		0	300	79.4	0	333	East	Medium	3
Late Cenomanian–Campanian		Mancos Shale		4,000	4,000	93.5	265	265	--	0	3
Middle-late Cenomanian		Dakota Sandstone		50	200	96.0	33	133	Northeast	Low	2
Early Cenomanian		Unconformity				98.5	0	0	Northeast	Medium	2
Albian		Cedar Mountain Formation		100	250	112.0	7	19	Northeast	Medium	2
Lower		Unconformity				145.0	0	0	Northeast	Medium	2
JURASSIC											
Oxfordian-Tithonian		Morrison Formation		600	800	154.0	60	80	Northeast	Medium	2
Middle		Unconformity (J5)				155.0	0	0	?	Low	1
Late Callovian	San Rafael	Summerville Formation		0	220	158.0	0	110	--	0	1
Middle Callovian	San Rafael	Curtis Formation		0	200	159.0	0	200	--	0	1
Callovian	San Rafael	Entrada Sandstone (Slick Rock Member)		100	500	161.0	50	250	?	Low	1
Late Bajocian–early Callovian	San Rafael	Carmel Formation–Entrada Sandstone (Dewey Bridge Member)		100	300	170.0	11	33	--	0	1
Aalenian		Unconformity (J2)				178.0	0	0	?	Low	1
Pliensbachian-Toarcian	Glen Canyon	Navajo Sandstone		0	450	187.0	0	50	?	Low	1
Sinemurian-Pliensbachian	Glen Canyon	Kayenta Formation		100	250	194.5	13	33	West	Medium	1
Sinemurian	Glen Canyon	Wingate Sandstone		300	300	203.5	33	33	Northwest-southwest?	Low	1
TRIASSIC											
Late		Unconformity				208.0	0	0	Northwest?	Low	1
Late		Chinle Formation		300	600	235.0	11	22	Northwest	Medium	1
Mid-Anisian		Unconformity				240.5	0	0	Northwest?	Low	1
Smithian		Moenkopi Formation		0	800	241.1	0	320	Northwest	Low	1
Dienerian		Moenkopi Formation (Hoskinnini Member)		50	50	243.4	125	125	?	Low	1
Early		Unconformity				245.0	0	0	East	Low	1
PERMIAN											
Late		Unconformity				256.1	0	0	West?	Low	1
Leonardian	Cutler	White Rim Sandstone		0	500	268.8	0	39	--	0	1

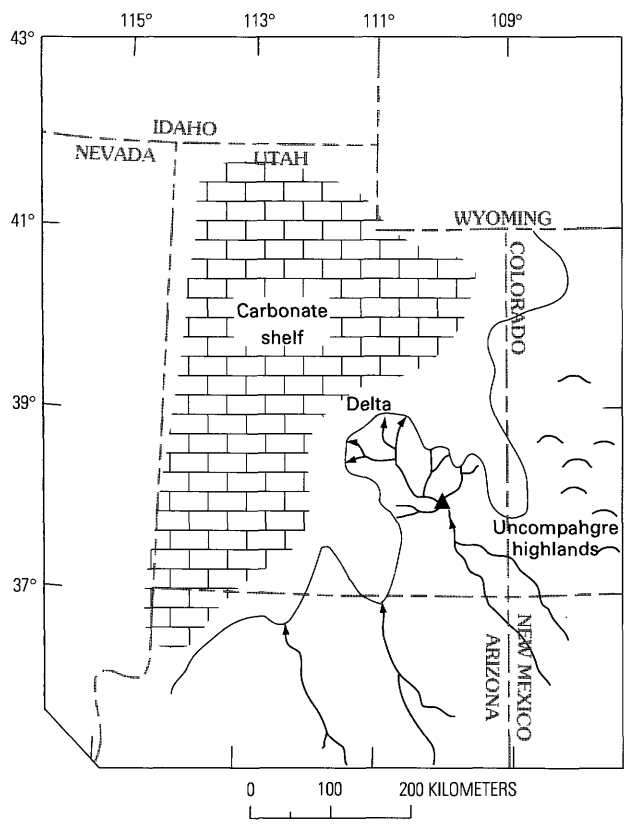

Figure 1. Paleogeography during deposition of the Torrey Member of the Lower Triassic Moenkopi Formation. Triangle indicates location of Tar Sand Triangle; arrows indicate direction of stream and inferred ground-water flow. Modified from Blakey (1974).

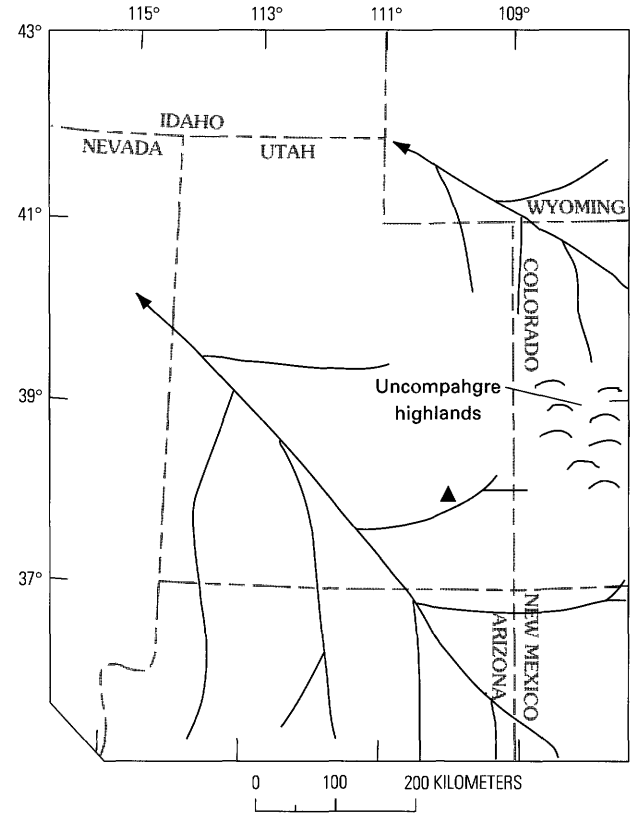

Figure 2. Paleogeography during deposition of the Shinarump Member of the Upper Triassic Chinle Formation. Triangle indicates location of Tar Sand Triangle; arrows indicate direction of stream and inferred ground-water flow. Modified from Dubiel (1989).

deposits (Molenaar, 1971). The marine Carmel, Curtis, and Summerville Formations indicate hydrostatic ground-water conditions (fig. 5). The dominantly eolian Entrada Sandstone represents erg and sabkha deposits. Hydraulic gradients during deposition of the San Rafael Group were the lowest since deposition of the Moenkopi. Sea water probably displaced fresh ground water introduced during fluvial episodes. The J5 unconformity represents the last stage of this period dominated by low gradients and northwest-southwest ground-water flow.

2. From the beginning of deposition of the Upper Jurassic Morrison Formation (155 Ma) through deposition of the middle to upper Cenomanian Dakota Sandstone (93.5 Ma) was a period (60 m.y.) characterized by moderate gradients and ground-water flow toward the northeast. Fluvial deposition and erosional periods favored recharge of fresh water and flushing of sea water and hypersaline brine.

The Morrison Formation in the Canyonlands area consists of a lower fluvial sandstone and an upper overbank and lacustrine mudstone (Craig and others, 1955; Tyler and Ethridge, 1983; Turner and Fishman, 1991). Current directions indicate northeastward and eastward flow of ground water (fig. 6). Highland areas of the Elko uplift (Thorman and others, 1991) were the source of ground-water recharge. Mixing of fresh water and underlying saline water in the shallow subsurface is indicated by uranium-vanadium deposits (Northrop and Goldhaber, 1990; Sanford, 1992).

Unconformably overlying the Morrison Formation are the Cedar Mountain and Burro Canyon Formations, which consist of fluvial sandstones shed from the Sevier highlands. The Cedar Mountain Formation, west of the Colorado River, exhibits eastward flow directions, whereas the Burro Canyon Formation, east the Colorado River, exhibits northerly and easterly flow directions (Craig, 1981).

Transgressive shoreline deposits of the Dakota Sandstone (Franczyk and others, 1992) mark the end of this period of dominantly northeastward flow (fig. 7). Fresh-water swamp and nearshore marine environments in the Dakota suggest discharge of fresh ground water and interaction with sea water typical of coastal regions.

3. The upper Cenomanian to Campanian Mancos Shale (93.5–76.6 Ma) was deposited in a shallow inland seaway (fig. 8). Because the Mancos and younger strata have been eroded from the Canyonlands area, reconstruction of ground-water flow requires interpolation from exposures to the north, south, and west. During this period, ground water

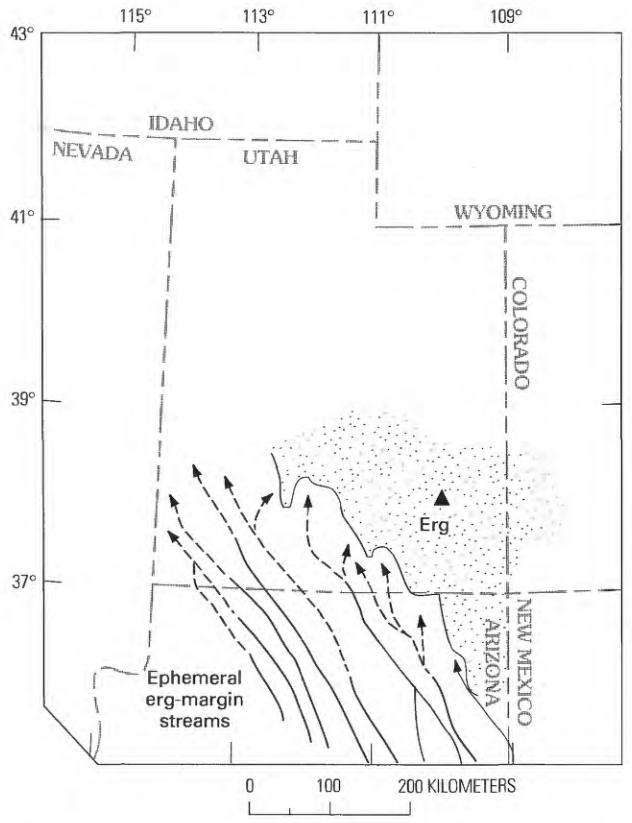

Figure 3. Paleogeography during deposition of the Lower Jurassic Wingate Sandstone. Triangle indicates location of Tar Sand Triangle; arrows indicate direction of stream and inferred ground-water flow. Modified from Clemmensen and others (1989).

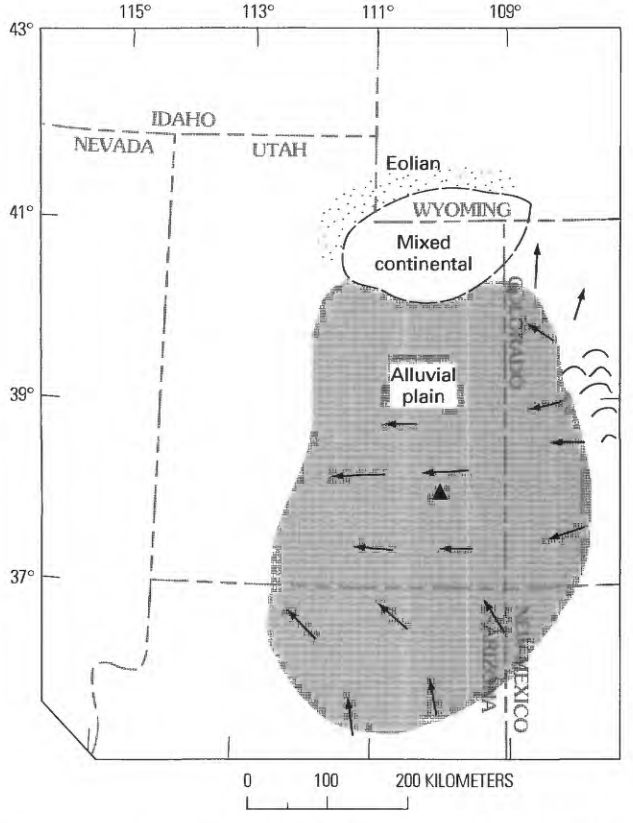

Figure 4. Paleogeography during deposition of the Lower Jurassic Kayenta Formation. Triangle indicates location of Tar Sand Triangle; arrows indicate direction of stream and inferred ground-water flow. Modified from Peterson (1988).

in sedimentary rocks below the Mancos was under hydrostatic conditions. Compaction of sub-Mancos sediments would have caused minor upward and outward flow, but compaction probably was minimal because of the abundance of sandstone in the section. The rapid deposition rate and the low permeability of Mancos sediments could have allowed overpressures to build up in the Mancos (Sanford, 1990). Pore water may have escaped downward into the Dakota as well as upward. The direction of compaction-driven flow can be estimated from isopachs of Upper Cretaceous rocks (fig. 8). If compaction-driven flow is mainly outward from the thickest part of a section, then it was mainly eastward and southeastward in the study area.

The Castlegate Sandstone represents a regressive period between the main body of the Mancos and the Buck Tongue of the Mancos. The Castlegate grades from fluvial to nearshore-marine sandstone (Fouch and others, 1983) and was probably mostly marine in the Canyonlands area. Ground-water flow was eastward. Hydraulic gradients would have been low, and ground water included both discharging fresh water and sea water. Owing to the low gradient, regional flow deeper in the section would have been minimal.

4. Regressive marine, coastal plain, and alluvial plain environments dominated in the late Campanian (Fouch and others, 1983; Franczyk and others, 1990) from 79.4 to 74 Ma. Fluvial deposits indicate eastward ground-water flow. This period was the second major period of topographically driven ground-water flow (the first being during Late Jurasssic–Early Cretaceous time).

The Sego Sandstone represents a microtidal barrier-island coastline environment (Franczyk and others, 1990). Gradients were near zero, and almost hydrostatic conditions prevailed. The Neslen Formation represents deposition in a meander plain by streams flowing northeast to southeast (Franczyk and others, 1990). Gradients were low, and the regional flow was generally eastward.

5. In the period from middle late Campanian to late Miocene (74–10 Ma), gradients were low to moderate, and flow was generally northward. Current directions changed from easterly in early late Campanian to northeasterly and northerly in late late Campanian time (fig. 9) (Franczyk and others, 1992).

The Farrer and Tuscher Formations represent meandering and braided river systems (Franczyk and others, 1990). Northeastward and northward current directions were probably influenced by uplift of the San Rafael Swell (Franczyk and others, 1990). Inferred topographically driven ground-water flow rates probably were moderate; northeasterly flow dominated during much of Farrer and

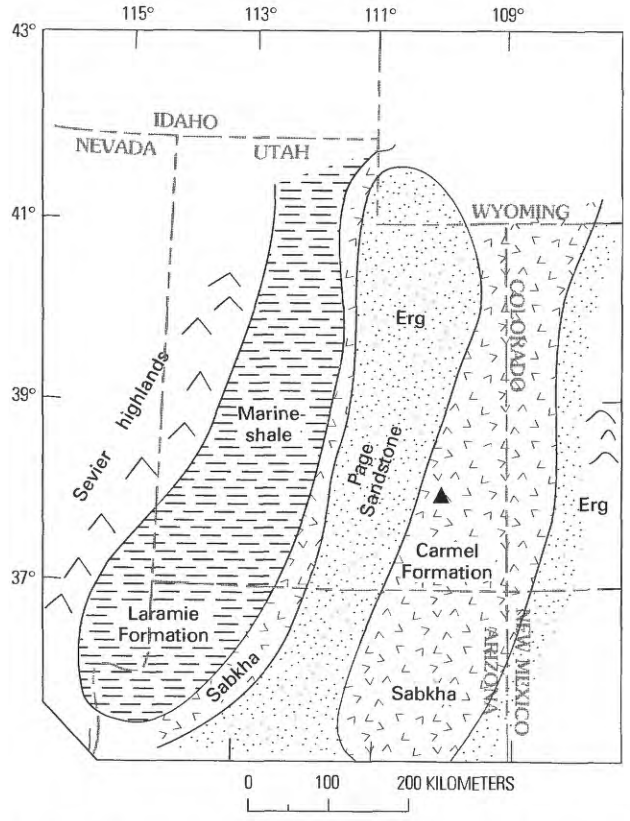

Figure 5. Paleogeography during deposition of the lower part of the Middle Jurassic Page Sandstone and Carmel Formations. Triangle indicates location of Tar Sand Triangle. Modified from Peterson (1988).

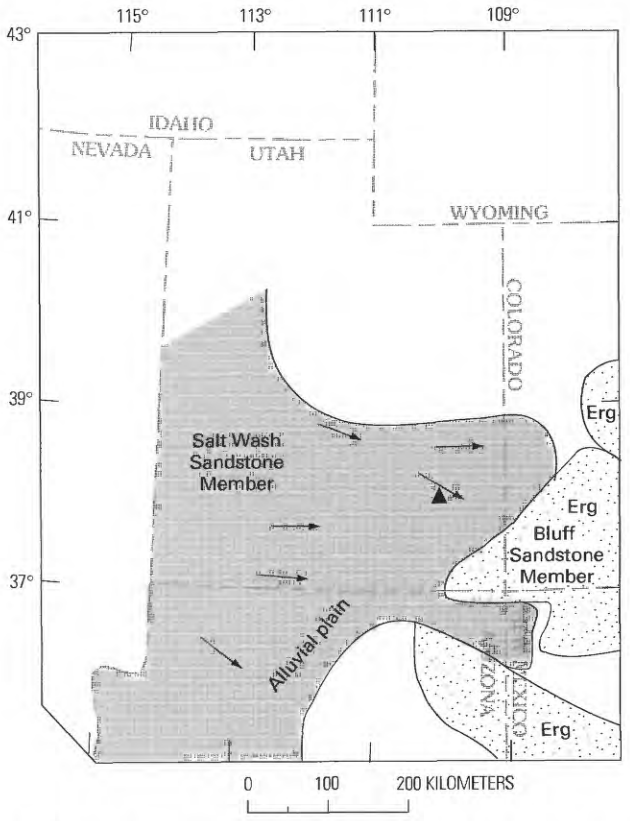

Figure 6. Paleogeography during deposition of the lower part of the Salt Wash and Bluff Sandstone Members of the Upper Jurassic Morrison Formation. Triangle indicates location of Tar Sand Triangle; arrows indicate direction of stream and inferred ground-water flow. Modified from Peterson (1988).

Tuscher, deposition, and northward flow dominated late in the deposition.

In the Canyonlands area Maastrichtian through middle Eocene time was characterized by slight uplift, low relief, and probably nondeposition (figs. 10, 11) (Franczyk and others, 1990). During deposition of the lower to middle Eocene part of the Wasatch Formation to the north, sediments were transported north to northwest between the San Rafael uplift and the Uncompahgre uplift (Franczyk and others, 1990). Inferred ground-water flow was moderate and directed northward to northwestward.

Little is known of the period from late Eocene to early Miocene (40–10 Ma). The northward drainage (fig. 12) must have reversed prior to cutting of the Grand Canyon, but the timing of the reversal is unknown. Southwest of the study area in Arizona, deposits as young as 20–18 Ma indicate northward drainage (Lucchitta, 1972). Deposits at the mouth of the Colorado River indicate that the river did not exist before 10.6 Ma (Lucchitta, 1972). Tectonic activity and lava flows from the upper Colorado also support a 10-Ma age for initiation of Colorado River downcutting (Larson and others, 1975). Thus, sometime between 20 and 10 Ma drainage changed from north to southwest. Meanders of the Colorado River indicate a low to moderate slope on the erosion surface prior to major downcutting. Ground-water flow is inferred to have been northward prior to 20 Ma and to have gradually changed to southwestward by 10 Ma.

6. The last distinctive phase in the topographic history was uplift of the Colorado Plateau and downcutting by the Colorado River (10 Ma to present) (Lucchitta, 1972; Larson and others, 1975). For the first time, large-scale erosion allowed many units to be drained of ground water. The regional flow system was broken up into local flow systems at least down to river level, which locally corresponds to the top of the Paradox Formation in the Canyonlands area. Ground water began to flow toward the Colorado River, westward in the east part of the area, southward in the north part of the area, and eastward in the west part of the area. Fresh ground water replaced some saline pore water. The high topographic gradients induced large ground-water flows that were limited by available recharge.

In summary, there were six distinctive periods of ground-water flow in the study area. (1) From Late Permian to Middle Jurassic (256–155 Ma), ground water flowed northwest with tributary flow southwest off the Uncompahgre uplift and some eastward flow immediately following the

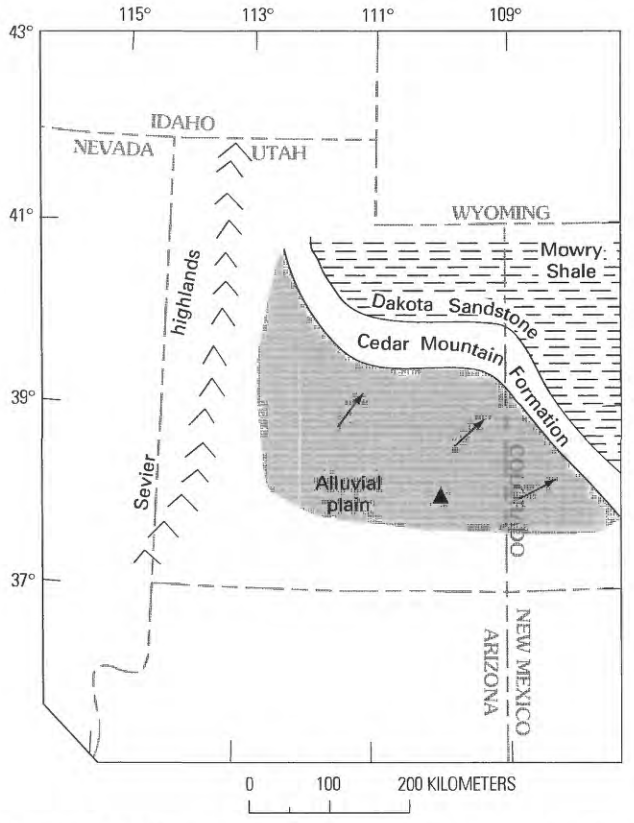

Figure 7. Paleogeography during the early Cenomanian *Neogastroplites americanus* faunal zone and deposition of parts of the Dakota Sandstone, Mowry Shale, and Cedar Mountain Formations. Triangle indicates location of Tar Sand Triangle; arrows indicate direction of stream and inferred ground-water flow. Modified from Franczyk and others (1992).

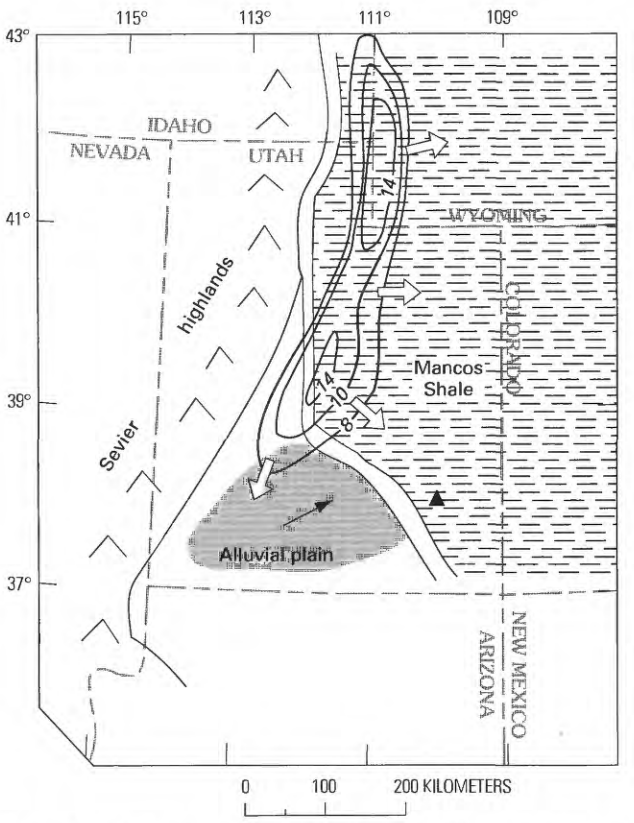

Figure 8. Paleogeography during the middle Coniacian *Inoceramus deformis* faunal zone and deposition of part of the Mancos Shale. Contours show thickness of Upper Cretaceous rocks (in thousands of feet), and open arrows show inferred direction of compaction-driven ground-water flow. Triangle indicates location of Tar Sand Triangle; arrow indicates direction of stream and inferred ground-water flow. Modified from Franczyk and others (1992).

Permian-Triassic unconformity. (2) From Late Jurassic to middle to late Cenomanian (155–93.5 Ma), ground water flowed northeast from the Elko and Sevier highlands. (3) From late Cenomanian to Campanian (93.5–76.6 Ma), the Mancos Shale was deposited, and conditions were almost hydrostatic. (4) During late Campanian (79.4–74 Ma), ground water flowed eastward from the Sevier highlands. (5) From middle late Campanian to late Miocene (74–10 Ma), flow was northward toward the Uinta Basin. (6) From late Miocene (10 Ma) to the present, flow was generally southwestward, but dissection by the Colorado River resulted in highly localized flows.

GROUND-WATER FLOW HISTORY

Knowing the topographic history and assuming that topographically driven ground-water flow parallels the topographic gradient and the surface-water direction, one can evaluate the effect of transmissivity variations along the flow path in the Canyonlands area. Specifically, it is necessary to determine the extent of vertical flow upward or downward because vertical flow affects the migration and trapping of petroleum. A semiquantitative analysis was performed using reconstructed topographic slopes, measured thicknesses, and hydraulic conductivities. As a first approximation, other factors being the same, decreasing transmissivity favors upward flow and discharge, and increasing transmissivity favors downward flow and recharge. Other factors affect ground-water flow, but there is little o r no data on them. For example, changes in topographic slope affect flow, but accurate values of paleoslope are usually unavailable. Thus, only changes in transmissivity are considered here. Thicknesses of units are reasonably well known, but hydraulic conductivities are more uncertain. Uncertainty results from two sources. First, measured hydraulic conductivities are highly variable. Variations of two orders of magnitude are common. Given the scarcity of measurements, systematic variations are difficult to ascertain. Average values for many units may mask real variations. Second, modern hydraulic conductivi-

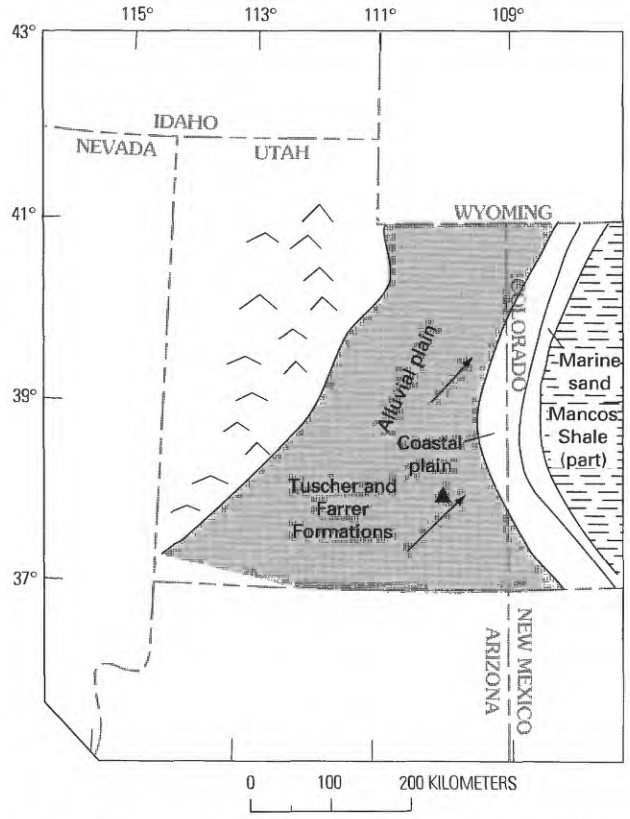

Figure 9. Paleogeography during the late late Campanian *Exiteloceras jenneyi* faunal zone and deposition of part of the Tuscher and Farrer Formations. Triangle indicates location of Tar Sand Triangle; arrows indicate direction of stream and inferred ground-water flow. Modified from Franczyk and others (1992).

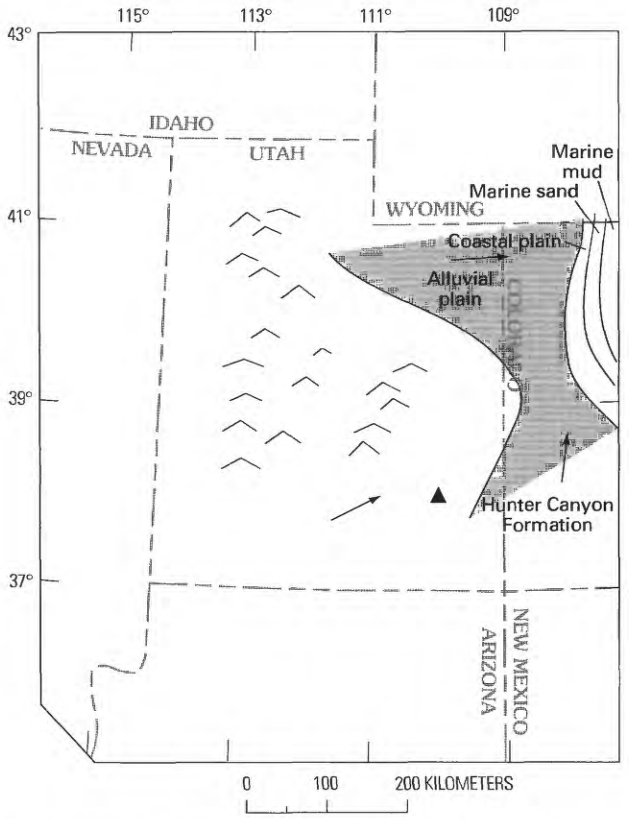

Figure 10. Paleogeography during the early Maastrichtian *Baculites reesidei* faunal zone and deposition of part of the Hunter Canyon Formation. Triangle indicates location of Tar Sand Triangle; arrows indicate direction of stream and inferred ground-water flow. Modified from Franczyk and others (1992).

ties probably have changed from those in the past. Compaction, fracturing, dissolution, and cementation have changed the permeability by unknown amounts.

To judge the significance of these uncertainties I analyzed the hydraulic history using three sets of data: (1) total thickness of the stratigraphic section, (2) thickness of aquifers, and (3) transmissivities of the stratigraphic section. Using thickness removes the effect of hydraulic conductivity. This approach has the advantages of removing the effect of uncertainty in hydraulic conductivity and relying only on the relatively well known thicknesses. The drawback is that it ignores real, but uncertain, variations in hydraulic conductivity. Another approximation is to consider the thickness of aquifers only. This approach emphasizes the main water-conducting units and may be a closer approximation to actual transmissivities than thickness of the entire sedimentary package, but it avoids the uncertainties of modern, measured hydraulic conductivities. Finally, using modern transmissivities calculated from thicknesses and measured hydraulic conductivities is the best approximation to past transmissivities, assuming there has been no change in hydraulic conductivity with time. The distribution of hydraulic conductivity is reasonably well known for major aquifers: the Madison-Redwall, Cutler-Maroon, and Weber-De Chelly (Geldon, in press).

The discrepancy between the three approaches approximates the error caused by uncertainty in past hydraulic conductivities. If the three approaches yield the same result, the result is more reliable than if the three approaches disagree.

The study area used for this semiquantitative analysis is within lat 37°30'–38°30' N. and long 109°–111° W. (fig. 13). The area was divided into 16 cells, 4 per side, for data digitizing, contouring, and calculation. Hydraulic data, listed in table 2, are shown in groups of 16 values corresponding to the 16 cells. The five columns in table 2 are (1) thickness of the individual unit, (2) transmissivity of the individual unit, (3) cumulative thickness up from the base of the section, (4) cumulative thickness of aquifers only from the base of the section, and (5) cumulative transmissivity from the base of the section. Principal sources of stratigraphic and hydrologic data are compilations by Geldon (in press) for Paleozoic rocks and by Freethey and Cordy (1991) for Mesozoic rocks. Thickness and hydraulic conductivity for hydrostratigraphic units were gridded from contour maps for areas where data are sufficient. For the deeper units, from the Cambrian Flathead-Tapeats aquifer to the Triassic Chinle-Moenkopi

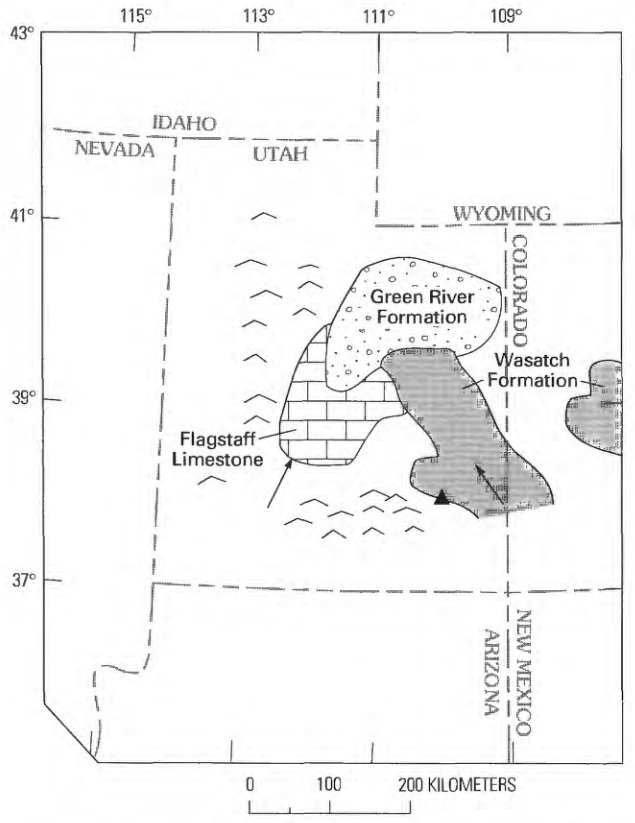

Figure 11. Paleogeography during the early Eocene and deposition of parts of the Wasatch and Green River Formations and Flagstaff Limestone. Triangle indicates location of Tar Sand Triangle; arrows indicate direction of stream and inferred ground-water flow. Modified from Franczyk and others (1992).

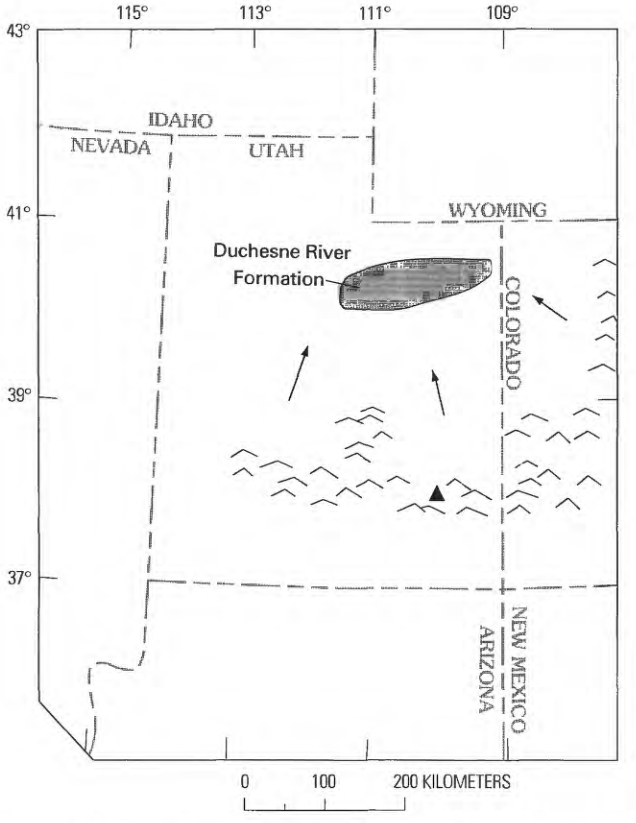

Figure 12. Paleogeography during the latest Eocene and (or) early Oligocene and deposition of the Duchesne River Formation. Triangle indicates location of Tar Sand Triangle; arrows indicate direction of stream and inferred ground-water flow. Modified from Franczyk and others (1992).

confining unit, isopach data are available for most of the study area. From the Lower Jurassic Navajo-Nugget aquifer to the Upper Cretaceous Dakota aquifer, the units have been eroded in places within the study area, and the missing data are supplied by interpolation. For the Upper Cretaceous Mesaverde aquifer and the Upper Cretaceous Mancos confining unit, both of which are eroded from the study area, average values of thickness and hydraulic conductivity are calculated from the nearest locations at which they are present. For major Paleozoic aquifers, hydraulic conductivity has been contoured for the entire study area (Geldon, in press). For less important aquifers and for confining units, a constant hydraulic conductivity was used and was the median of the values in and near the study area. For Mesozoic aquifers (Freethey and Cordy, 1991), transmissivity has been contoured over the study area, and hydraulic conductivity was calculated from these values. For Mesozoic confining units, mean hydraulic conductivities are from figure 40 of Freethey and Cordy (1991). Where data are missing, permeability in air (figure 32 of Freethey and Cordy, 1991) was converted to hydraulic conductivity by multiplying by the factor 0.003 m/day/mD (0.01 ft/day/mD). This factor is the mean of the hydraulic conductivity to permeability ratio for those units for which both hydraulic conductivity and permeability are available.

Hydraulic properties of the section below the Permian White Rim Sandstone are controlled by three groups of hydrostratigraphic units: the lower Paleozoic section from the Cambrian Flathead-Tapeats aquifer to the Upper Mississippian to Middle Pennsylvanian Belden-Molas confining unit, the Lower Mississippian to Middle Pennsylvanian Paradox confining unit, and the Lower Pennsylvanian to Lower Permian Cutler-Maroon aquifer. Deposition of the lower Paleozoic section established the initial distribution of thickness, which increased regularly across the study area from southeast to northwest. The Upper Devonian to lower Upper Mississippian Madison-Redwall aquifer (consisting of the Mississippian Leadville Limestone in the study area) within this section provided most of the transmissivity. Transmissivity in the Leadville Limestone varies by two orders of magnitude in the Canyonlands area, from about 1×10^{-6} to 2×10^{-4} m^2/s (1–200 ft^2/day, Geldon, in press). One highly transmissive area is in the White Canyon–Gypsum Canyon area southeast of the Colorado River, and another is west of the

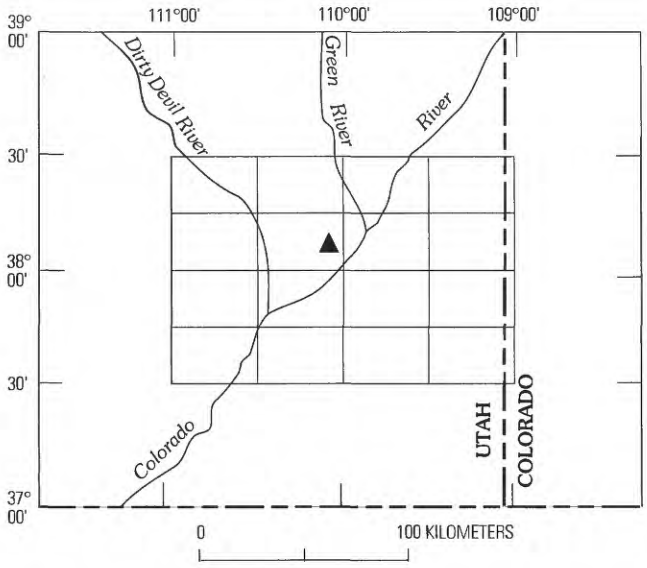

Figure 13. Grid used for analysis of the hydrology of the Canyonlands area. Triangle indicates location of Tar Sand Triangle.

Dirty Devil River northwest of the Colorado River. The complexity of the transmissivity distribution and the magnitude of the variations makes difficult any generalizations for the area as a whole.

The Paradox Formation superimposed an irregular thickness distribution on the preexisting relatively regular distribution in that it added a "ridge" of thick sediments across the north-central part of the study area. Thickness decreased both north and south from this ridge. This feature subsequently dominated the entire section.

Deposition of the Lower Permian Cutler Group added a wedge of sediment that thinned from the Uncompahgre uplift in the northeast to the southwest. The most transmissive zone forms a "ridge" trending northeast across the study area. Transmissivity values range from about 3×10^{-6} to 1×10^{-4} m^2/s (3–100 ft^2/day, Geldon, in press).

At the end of deposition of the White Rim Sandstone total thickness of the section up through the White Rim Sandstone varied from about 1,600 to 2,300 m (5,200–7,500 ft), aquifer thickness from about 1,100 to 1,500 m (3,600–4,900 ft), and cumulative transmissivity from about 5×10^{-5} to 5×10^{-4} m^2/s (table 2). The section thins both north and south from the Paradox-controlled north-central thick area. Aquifer thickness increases to the north and east from the southeastern corner. Transmissivity decreases south and east from the northwestern corner and decreases east, west, and north from a south-central transmissive zone. The discrepancies among the three approaches indicate that the uncertainties equal the natural variations in magnitude. Whether ground-water flow was southwestward off the Uncompahgre uplift, westward off the Monument uplift, or eastward off a local high, both upward and downward flow probably occurred locally in various parts of the study area.

At the end of deposition of the Upper Triassic Chinle Formation, total thickness of the section varied from about 1,900 to 2,400 m (6,200–7,900 ft), aquifer thickness from about 1,100 to 1,500 m (3,600–4,900 ft), and cumulative transmissivity from 3×10^{-4} to 1×10^{-3} m^2/s (table 2). Thickness distribution is similar to that at the end of deposition of the White Rim Sandstone. Total thickness decreases north and south from a north-central thick area. Aquifer thickness is the same as at the end of deposition of the White Rim Sandstone. Transmissivity decreases from the southwest toward the northeast and varies considerably within the area. As indicated by fluvial sandstones in the Lower and Middle(?) Triassic Moenkopi Formation and Upper Triassic Chinle Formation, ground-water flow was dominantly northwestward. Vertical flow based on variations in total thickness and aquifer thickness suggests recharge followed by discharge along the northwestward flow path. Vertical flow based on transmissivity suggests more variable recharge and discharge but slight net discharge. Again, the discrepancies among the three approaches indicate uncertainties having similar magnitude as the natural variations. For northwestward ground-water flow during deposition of the overlying Lower Jurassic Wingate Sandstone, the transmissivity suggests slight discharge; however, the total thickness is constant.

At the end of deposition of the Lower Jurassic Navajo Sandstone, total thickness of the section varied from about 2,150 to 2,800 m (7,100–9,200 ft), aquifer thickness from about 1,350 to 1,900 m (4,400–6,200 ft), and transmissivity from 6×10^{-4} to 2×10^{-3} m^2/s (table 2). Thickness distribution is essentially similar to that in the two periods previously discussed. Aquifer thickness decreases from the southwestern corner northward and especially eastward. Transmissivity decreases strongly from the northwestern corner to the southeastern corner. The gradient of decreasing transmissivity thus changed from northward and northeastward at the end of Chinle deposition to southeastward at the end of Navajo deposition. This change is mostly due to the thickness of the Navajo Sandstone, which thins dramatically from west to east (Jobin, 1962). During the period of marine, sabkha, and eolian deposition that followed deposition of the Navajo, topographic gradients were slight to nil and recharge was low. Ground-water flow was probably dominated by shoreline-related processes such as evaporation, sea-water refluxing, and density-driven convection. Regional flow in aerially exposed areas was probably toward the sea that invaded from the northwest. Although the total thickness variation is slight, increasing transmissivity in this direction suggests that ground water recharged into the Navajo-Nugget aquifer.

At the end of deposition of the Middle Jurassic Carmel Formation, total thickness of the section varied from about 2,200 to 2,800 m (7,200–9,200 ft) and transmissivity from 9.5×10^{-4} to 2.6×10^{-3} m^2/s (table 2). Aquifer thickness

Table 2. Hydraulic properties of units in Canyonlands area.
[Each block of 16 corresponds to the grid in figure 13]

Thickness (meters)				Transmissivity of unit (m^2/sec)				Total thickness (meters)				Aquifer thickness (meters)				Cumulative transmissivity from base of section (m^2/sec)			
MESAVERDE AQUIFER																			
610	610	610	610	8.60E-04	8.60E-04	8.60E-04	8.60E-04	4,145	4,087	4,093	3,932	2,545	2,545	2,545	2,463	4.25E-03	2.51E-03	3.19E-03	2.06E-03
610	610	610	610	8.60E-04	8.60E-04	8.60E-04	8.60E-04	4,459	4,456	4,301	4,426	2,853	2,728	2,725	2,444	3.78E-03	2.41E-03	2.44E-03	2.02E-03
610	610	610	610	8.60E-04	8.60E-04	8.60E-04	8.60E-04	4,289	4,182	4,112	3,828	2,780	2,536	2,527	2,240	3.29E-03	2.59E-03	2.38E-03	1.90E-03
610	610	610	610	8.60E-04	8.60E-04	8.60E-04	8.60E-04	4,142	4,093	4,087	3,917	2,761	2,527	2,505	2,268	2.38E-03	2.61E-03	2.21E-03	2.14E-03
MANCOS CONFINING UNIT																			
610	610	610	610	1.08E-04	1.08E-04	1.08E-04	1.08E-04	3,536	3,478	3,484	3,322					3.39E-03	1.65E-03	2.33E-03	1.20E-03
610	610	610	610	1.08E-04	1.08E-04	1.08E-04	1.08E-04	3,850	3,847	3,691	3,816					2.92E-03	1.55E-03	1.58E-03	1.16E-03
610	610	610	610	1.08E-04	1.08E-04	1.08E-04	1.08E-04	3,679	3,572	3,502	3,219					2.43E-03	1.73E-03	1.52E-03	1.04E-03
610	610	610	610	1.08E-04	1.08E-04	1.08E-04	1.08E-04	3,533	3,484	3,478	3,307					1.52E-03	1.75E-03	1.35E-03	1.28E-03
DAKOTA AQUIFER																			
30	40	40	52	5.38E-06	1.08E-05	1.61E-05	2.15E-05	2,926	2,868	2,874	2,713	1,935	1,935	1.935	1,853	3.28E-03	1.55E-03	2.23E-03	1.10E-03
30	40	40	52	5.38E-06	2.15E-05	5.38E-05	5.38E-05	3,240	3,237	3,082	3,206	2,243	2,118	2,115	1,835	2.18E-03	1.45E-03	1.47E-03	1.05E-03
30	40	40	52	5.38E-06	5.38E-05	1.08E-04	1.08E-04	3,069	2,963	2,893	2,609	2,170	1,926	1917	1,631	2.32E-03	1.62E-03	1.42E-03	9.31E-04
30	40	40	52	5.38E-06	5.38E-05	1.08E-04	1.29E-04	2,923	2,874	2,868	2,697	2,152	1,917	1,896	1,658	1.42E-03	1.64E-03	1.25E-03	1.17E-03
MORRISON CONFINING UNIT																			
61	79	98	116	8.60E-06	1.12E-05	1.38E-05	1.63E-05	2,896	2,829	2,835	2,661					3.27E-03	1.54E-03	2.21E-03	1.07E-03
52	79	98	122	7.31E-06	1.12E-05	1.38E-05	1.72E-05	3,210	3,197	3,042	3,155					2.80E-03	1.42E-03	1.42E-03	9.98E-04
40	82	101	113	5.59E-06	1.16E-05	1.42E-05	1.59E-05	3,039	2,923	2853	2,557					2.32E-03	1.57E-03	1.31E-03	8.23E-04
30	82	104	91	4.30E-06	1.16E-05	1.46E-05	1.29E-05	2,893	2,835	2,829	2,646					1.41E-03	1.59E-03	1.14E-03	1.04E-03
MORRISON AQUIFER																			
91	91	91	91	7.53E-05	7.53E-05	5.38E-05	3.23E-05	2,835	2,749	2,737	2,545	1,905	1,896	1,896	1,801	3.26E-03	1.52E-03	2.20E-03	1.06E-03
110	110	107	107	5.38E-05	1.08E-04	7.53E-05	3.23E-05	3,158	3,118	2,944	3,033	2,213	2,079	2076	1,783	2.80E-03	1.41E-03	1.41E-03	9.81E-04
146	137	128	122	4.30E-05	7.53E-05	5.38E-05	3.23E-05	2,999	2,841	2,752	2,444	2,140	1,887	1,878	1,579	2.31E-03	1.56E-03	1.29E-03	8.08E-04
158	134	113	91	4.30E-05	5.38E-05	5.38E-05	9.68E-05	2,862	2,752	2,725	2,554	2,121	1,878	1,856	1,606	1.41E-03	1.57E-03	1.12E-03	1.03E-03
SUMMERVILLE-CURTIS CONFINING UNIT																			
107	55	43	30	2.45E-04	1.26E-04	9.78E-05	6.99E-05	2,743	2,658	2,646	2,454					3.19E-03	1.45E-03	2.14E-03	1.03E-03
91	70	52	30	2.10E-04	1.61E-04	1.19E-04	6.99E-05	3,048	3,008	2,838	2,926					2.74E-03	1.31E-03	1.33E-03	9.48E-04
61	70	52	30	1.40E-04	1.61E-04	1.19E-04	6.99E-05	2,853	2,704	2,624	2,323					2.27E-03	1.48E-03	1.24E-03	7.75E-04
46	40	34	30	1.05E-04	9.09E-05	7.69E-05	6.99E-05	2,704	2,618	2,612	2,463					1.36E-03	1.52E-03	1.07E-03	9.32E-04
ENTRADA-PREUSS AQUIFER																			
183	140	140	101	6.45E-04	4.30E-04	2.15E-04	7.53E-05	2,637	2,603	2,603	2,423	1,814	1,804	1,804	1,710	2.94E-03	1.32E-03	2.05E-03	9.56E-04
183	140	140	98	2.15E-04	1.72E-04	1.29E-04	8.60E-05	2,957	2,938	2,786	2,896	2,103	1,969	1,969	1,676	2.53E-03	1.14E-03	1.21E-03	8.79E-04
195	152	152	110	1.08E-04	1.08E-04	1.08E-04	1.08E-04	2,792	2,633	2,573	2,292	1,993	1,750	1,750	1,457	2.13E-03	1.32E-03	1.12E-03	7.05E-04
213	165	165	113	4.30E-05	9.68E-05	1.51E-04	2.15E-04	2,658	2,579	2,579	2,432	1,963	1,743	1,743	1,515	1.26E-03	1.43E-03	9.94E-04	8.63E-04
CARMEL CONFINING UNIT																			
79	30	30	30	2.80E-05	1.08E-05	1.08E-05	1.08E-05	2,454	2,463	2,463	2,323					2.30E-03	8.93E-04	1.83E-03	8.81E-04
61	30	30	30	2.15E-05	1.08E-05	1.08E-05	1.08E-05	2,774	2,798	2,646	2,798					2.32E-03	9.73E-04	1.08E-03	7.93E-04
61	30	30	30	2.15E-05	1.08E-05	1.08E-05	1.08E-05	2,597	2,481	2,420	2,182					2.02E-03	1.21E-03	1.01E-03	5.98E-04
61	30	30	30	2.15E-05	1.08E-05	1.08E-05	1.08E-05	2,444	2,414	2,414	2,320					1.22E-03	1.33E-03	8.43E-04	6.47E-04

Table 2. Hydraulic properties of units in Canyonlands area—Continued.

Thickness (meters)				Transmissivity of unit (m^2/sec)				Total thickness (meters)				Aquifer thickness (meters)				Cumulative transmissivity from base of section (m^2/sec)			
NAVAJO-NUGGET AQUIFER																			
396	366	366	335	1.61E-03	3.23E-04	1.08E-03	5.38E-04	2,374	2,432	2,432	2,292	1,631	1,664	1,664	1,609	2.27E-03	8.82E-04	1.82E-03	8.70E-04
427	396	396	335	1.61E-03	3.23E-04	5.38E-04	4.30E-04	2,713	2,768	2,615	2,768	1,920	1,829	1,829	1,579	2.30E-03	9.62E-04	1.07E-03	7.82E-04
396	335	335	274	1.40E-03	3.23E-04	3.23E-04	1.08E-04	2,536	2,451	2,390	2,152	1,798	1,597	1,597	1,347	2.00E-03	1.20E-03	1.00E-03	5.87E-04
396	335	335	305	6.45E-04	3.23E-04	1.08E-04	8.60E-05	2,384	2,384	2,384	2,289	1,750	1,579	1,579	1,402	1.20E-03	1.32E-03	8.32E-04	6.37E-04
CHINLE-MOENKOPI CONFINING UNIT																			
274	305	305	152	4.84E-04	5.38E-04	5.38E-04	2.69E-04	1,978	2,067	2,067	1,957					6.58E-04	5.60E-04	7.44E-04	3.32E-04
305	305	152	152	5.38E-04	5.38E-04	2.69E-04	2.69E-04	2,286	2,371	2,219	2,432					6.85E-04	6.39E-04	5.34E-04	3.52E-04
305	305	244	244	5.38E-04	5.38E-04	4.30E-04	4.30E-04	2,140	2,115	2,054	1,878					6.01E-04	8.82E-04	6.81E-04	4.80E-04
274	305	305	274	4.84E-04	5.38E-04	5.38E-04	4.84E-04	1,987	2,048	2,048	1,984					5.50E-04	1.00E-03	7.25E-04	5.51E-04
WEBER-DE CHELLY AQUIFER																			
244	152	152	61	1.08E-04	5.38E-07	8.60E-05	1.08E-05	1,704	1,762	1,762	1,804	1,234	1,298	1,298	1,274	1.74E-04	2.20E-05	2.06E-04	6.36E-05
152	61	61	30	1.08E-05	1.08E-06	1.08E-04	8.60E-06	1,981	2,067	2,067	2,280	1,494	1,433	1,433	1,244	1.47E-04	1.02E-04	2.66E-04	8.29E-05
134	61	61	61	1.08E-06	1.08E-04	1.08E-04	5.38E-06	1,835	1,811	1,811	1,634	1,402	1,262	1,262	1,073	6.31E-05	3.44E-04	2.51E-04	4.95E-05
104	61	61	61	5.38E-06	2.15E-05	1.08E-04	3.23E-06	1,713	1,743	1,743	1,710	1,353	1,244	1,244	1,097	6.60E-05	4.62E-04	1.87E-04	6.68E-05
CUTLER-MAROON AQUIFER																			
244	671	671	823	3.23E-06	1.08E-05	8.60E-05	1.08E-05	1,460	1,609	1,609	1,743	991	1,146	1,146	1,213	6.67E-05	2.14E-05	1.20E-04	5.28E-05
610	792	792	762	2.15E-05	8.60E-05	1.08E-04	8.60E-06	1,829	2,006	2,006	2,249	1,341	1,372	1,372	1,213	1.36E-04	1.01E-04	1.58E-04	7.43E-05
701	762	762	640	5.38E-05	1.08E-04	1.08E-04	1.08E-05	1,701	1,750	1,750	1,573	1,268	1,201	1,201	1,012	6.20E-05	2.36E-04	1.44E-04	4.41E-05
792	762	762	701	5.38E-05	1.08E-04	5.38E-05	3.23E-05	1,609	1,682	1,682	1,649	1,250	1,183	1,183	1,036	6.06E-05	4.41E-04	7.98E-05	6.36E-05
PARADOX-EAGLE VALLEY CONFINING UNIT																			
122	152	152	305	4.30E-06	5.38E-06	1.08E-05	3.23E-05	1,216	939	939	920					6.35E-05	1.07E-05	3.44E-05	4.21E-05
61	305	305	762	2.15E-06	1.08E-05	2.69E-05	5.38E-05	1,219	1,213	1,213	1,487					1.15E-04	1.46E-05	5.06E-05	6.57E-05
91	213	213	366	3.23E-06	7.53E-06	1.29E-05	2.15E-05	1,000	988	988	933					8.27E-06	1.29E-04	3.61E-05	3.33E-05
61	213	213	366	2.15E-06	7.53E-06	1.29E-05	1.94E-05	817	920	920	948					6.85E-06	3.33E-04	2.60E-05	3.14E-05
BELDEN-MOLAS CONFINING UNIT																			
152	55	55	12	2.69E-06	9.68E-07	2.15E-07	5.38E-09	1,094	786	786	616					5.92E-05	5.29E-06	2.37E-05	9.83E-06
183	67	67	61	3.23E-06	1.18E-06	1.08E-06	2.15E-07	1,158	908	908	725					1.13E-04	3.81E-06	2.37E-05	1.19E-05
152	122	122	55	2.69E-06	2.15E-06	9.68E-07	5.38E-07	908	774	774	567					5.05E-06	1.21E-04	2.32E-05	1.18E-05
152	128	128	91	2.69E-06	2.26E-06	1.61E-06	7.53E-07	756	707	707	582					4.70E-06	3.26E-04	1.31E-05	1.20E-05
MADISON-REDWALL AQUIFER																			
320	244	244	213	5.38E-05	2.15E-06	2.15E-05	8.60E-06	942	732	732	604	747	475	475	390	5.65E-05	4.33E-06	2.34E-05	9.82E-06
305	250	250	183	1.08E-04	1.08E-06	1.08E-05	1.08E-05	975	841	841	664	732	579	579	451	1.09E-04	2.63E-06	2.27E-05	1.17E-05
274	244	244	189	1.08E-06	1.08E-04	1.08E-05	1.08E-05	756	652	652	512	567	439	439	372	2.36E-06	1.19E-04	2.22E-05	1.13E-05
250	232	232	189	1.08E-06	2.15E-04	1.08E-05	1.08E-05	604	579	579	491	457	421	421	335	2.01E-06	3.23E-04	1.15E-05	1.12E-05
ELBERT-PARTING CONFINING UNIT																			
73	73	73	61	1.08E-06	1.08E-06	1.08E-06	3.23E-07	622	488	488	390					2.77E-06	2.18E-06	1.94E-06	1.22E-06
91	79	79	76	1.08E-07	1.08E-07	1.08E-05	1.08E-07	671	591	591	482					1.85E-06	1.55E-06	1.19E-05	9.66E-07
98	91	91	79	1.08E-07	1.08E-05	1.08E-05	1.08E-08	482	408	408	323					1.28E-06	1.16E-05	1.15E-05	5.35E-07
85	98	98	79	1.08E-07	1.08E-04	1.08E-07	1.08E-08	354	347	347	302					9.33E-07	1.08E-04	7.42E-07	4.92E-07

Table 2. Hydraulic properties of units in Canyonlands area—Continued.

Thickness (meters)			Transmissivity of unit (m^2/sec)			Total thickness (meters)			Aquifer thickness (meters)			Cumulative transmissivity from base of section (m^2/sec)		
BIGHORN-MUAV AQUIFER														
366	183	122	1.29E-06	6.45E-07	4.30E-07	549	415	415	427	232	232	1.69E-06	1.10E-06	8.60E-07
366	274	195	1.29E-06	9.68E-07	6.88E-07	579	512	512	427	329	329	1.74E-06	1.45E-06	1.16E-06
213	122	91	7.53E-07	4.30E-07	3.23E-07	384	317	317	293	195	195	1.17E-06	8.77E-07	7.40E-07
110	91	55	3.87E-07	3.23E-07	1.94E-07	268	250	250	207	189	189	8.26E-07	7.61E-07	6.34E-07
GROS VENTRE–BRIGHT ANGEL CONFINING UNIT														
122	183	152	1.89E-07	2.84E-07	2.37E-07	183	232	232				4.04E-07	4.56E-07	4.30E-07
152	183	137	2.37E-07	2.84E-07	2.13E-07	213	238	238				4.52E-07	4.77E-07	4.71E-07
91	122	61	1.42E-07	1.89E-07	9.46E-08	171	195	195				4.22E-07	4.47E-07	4.17E-07
61	61	76	9.46E-08	9.46E-08	1.18E-07	158	158	158				4.39E-07	4.39E-07	4.41E-07
FLATHEAD-TAPEATS AQUIFER														
61	49	55	2.15E-07	1.72E-07	1.94E-07	61	49	49	61	49	49	2.15E-07	1.72E-07	1.94E-07
61	55	73	2.15E-07	1.94E-07	2.58E-07	61	55	55	61	55	55	2.15E-07	1.94E-07	2.58E-07
79	73	91	2.80E-07	2.58E-07	3.23E-07	79	73	73	79	73	73	2.80E-07	2.58E-07	3.23E-07
98	98	91	3.44E-07	3.44E-07	3.23E-07	98	98	98	98	98	98	3.44E-07	3.44E-07	3.23E-07
BIGHORN-MUAV AQUIFER														
366	183	122	1.29E-06	6.45E-07	4.30E-07	549	415	415	427	232	232	1.69E-06	1.10E-06	8.60E-07
366	274	195	1.29E-06	9.68E-07	6.88E-07	579	512	512	427	329	329	1.74E-06	1.45E-06	1.16E-06
213	122	91	7.53E-07	4.30E-07	3.23E-07	384	317	317	293	195	195	1.17E-06	8.77E-07	7.40E-07
110	91	55	3.87E-07	3.23E-07	1.94E-07	268	250	250	207	189	189	8.26E-07	7.61E-07	6.34E-07
GROS VENTRE–BRIGHT ANGEL CONFINING UNIT														
122	183	152	1.89E-07	2.84E-07	2.37E-07	183	232	232				4.04E-07	4.56E-07	4.30E-07
152	183	137	2.37E-07	2.84E-07	2.13E-07	213	238	238				4.52E-07	4.77E-07	4.71E-07
91	122	61	1.42E-07	1.89E-07	9.46E-08	171	195	195				4.22E-07	4.47E-07	4.17E-07
61	61	76	9.46E-08	9.46E-08	1.18E-07	158	158	158				4.39E-07	4.39E-07	4.41E-07
FLATHEAD-TAPEATS AQUIFER														
61	49	55	2.15E-07	1.72E-07	1.94E-07	61	49	49	61	49	49	2.15E-07	1.72E-07	1.94E-07
61	55	73	2.15E-07	1.94E-07	2.58E-07	61	55	55	61	55	55	2.15E-07	1.94E-07	2.58E-07
79	73	91	2.80E-07	2.58E-07	3.23E-07	79	73	73	79	73	73	2.80E-07	2.58E-07	3.23E-07
98	98	91	3.44E-07	3.44E-07	3.23E-07	98	98	98	98	98	98	3.44E-07	3.44E-07	3.23E-07

remained the same. Because of the relative thinness of this unit, hydraulic properties of the section were essentially unchanged from the previous period.

At the end of deposition of the Middle Jurassic Entrada Sandstone, total thickness of the section varied from about 2,300 to 3,000 m (7,500–9,800 ft), aquifer thickness from about 1,450 to 2,100 m (4,800–6,900 ft), and transmissivity from 7×10^{-4} to 3×10^{-3} m^2/s (table 2). Cumulative thickness retains the same general pattern exhibited since the Late Permian; however, the northwestward increase in transmissivity that started with deposition of the Navajo Sandstone is further accentuated by deposition of the Entrada Sandstone. This variation in transmissivity had little effect on the immediately subsequent flow system because marine conditions dominated the depositional period of the Middle Jurassic Summerville and Curtis Formations.

At the end of deposition of the Summerville Formation, total thickness of the section varied from about 2,300 to 3,050 m (5,500–10,000 ft) and transmissivity from 8×10^{-4} to 3×10^{-3} m^2/s (table 2). Owing to the thinness of the Curtis and Summerville, hydraulic properties of the total section changed only very slightly.

At the end of deposition of the Upper Jurassic Morrison aquifer (Salt Wash Member), total thickness of the section varied from about 2,400 to 3,200 m (7,900–10,500 ft), aquifer thickness from about 1,600 to 2,200 m (5,200–7,200 ft), and transmissivity from 8×10^{-4} to 3×10^{-3} m^2/s (table 2). Again, the relatively thin unit had little effect on the hydraulic properties; however, the Morrison Formation represents a major change in topographic slope. Although the Early and Middle Jurassic were dominated by low-slope marine, sabkha, and eolian environments, the Late Jurassic exhibited a dominant northeast slope that persisted until the early late Cenomanian. In this northeast direction, total thickness, aquifer thickness, and transmissivity all decrease and indicate ground-water discharge.

It is instructive to consider flow through the White Rim Sandstone during this period of northeastward ground-water flow. It is necessary to determine if conclusions for the section as a whole apply to the White Rim Sandstone, which was in the subsurface at this time. I consider the hydraulic properties for the section up through the White Rim and attempt to determine if there was exchange with the section above the White Rim. Gradients from southwest to northeast for the part of the section up through the White Rim increase for total thickness, decrease slightly for aquifer thickness, and increase for transmissivity; thus, there is no clear evidence for any systematic variation in thickness or transmissivity. This suggests that there was little exchange between the sections above and below the White Rim Sandstone. Thus, flow through the White Rim apparently was virtually horizontal as near as can be determined. Because the thinning of the total section and the aquifers below the Morrison mostly reflects the Navajo Sandstone, it is likely that discharge through the Morrison Formation came from the

Navajo Sandstone and did not affect the White Rim Sandstone. The same can be said for the whole period dominated by northeastward flow from Late Jurassic through Cenomanian time.

At the end of deposition of the Morrison confining unit (Brushy Basin Member), total thickness of the section varied from about 2,600 to 3,200 m (8,500–10,500 ft), and transmissivity from 8×10^{-4} to 3×10^{-3} m^2/s (table 2). Topographic slope was still to the northeast, and ground-water flow was essentially the same as during deposition of the Salt Wash Member, although the lower slope suggests slower flow rates.

At the end of deposition of the Upper Cretaceous Dakota aquifer, total thickness of the section varied from about 2,600 to 3,200 m (8,500–10,500 ft), aquifer thickness from about 1,600 to 2,200 m (5,200–7,200 ft), and transmissivity from 9×10^{-4} to 3×10^{-3} m^2/s (table 2). Flow conditions were relatively the same for the time period from deposition of the Salt Wash Member through deposition of the Dakota Sandstone except for some variations due to changes in slope.

At the end of deposition of the Upper Cretaceous Mancos confining unit, total thickness of the section had increased by about 600 m (2,000 ft) (table 2). Because all of the Mancos has been removed from the study area, there is no way to evaluate variations in thickness or transmissivity. Compaction may have been the most important driving force for ground-water flow, although even the maximum compaction-driven flow would be some two to four orders of magnitude less than gravity-driven flow (Sanford, 1990). Compaction-driven flow would have been upward and outward.

By the end of deposition of the Upper Cretaceous Mesaverde Group, approximately another 600 m (2,000 ft) of section was added, all of which has been removed by erosion. Ground-water flow was dominantly to the east during most of the deposition of the Mesaverde except for the final stages during deposition of the Campanian and Maastrichtian Farrer and Tuscher Formations when flow was north-northeast and north (Franczyk and others, 1992). Because of the lack of data for the Mancos and Mesaverde, it is impossible to evaluate variations in thickness and transmissivity of the total section; however, it is possible to evaluate the effect of eastward ground-water flow on the section that is preserved and focus on flow above and below the White Rim Sandstone. From west to east, total thickness increases, aquifer thickness decreases, and cumulative transmissivity is variable. Because of the discrepancies among the three approaches and the local variations, it is difficult to determine any consistent pattern. As well as can be determined, ground-water flow was horizontal, and there was little significant exchange between units above and below the White Rim Sandstone.

PENNSYLVANIAN-PERMIAN AQUIFERS

In order for petroleum to move from the source to the reservoir there must be a permeable pathway. The most favorable pathways for oil to reach the Tar Sand Triangle are sandstone units in hydrologic continuity with the White Rim Sandstone. A map of hydrologically connected Pennsylvanian and Permian sandstone aquifers constructed from numerous sources (principally Baars, 1962; Blakey and others, 1988; Hintze, 1988; Geldon, in press) shows that the White Rim was potentially in hydrologic communication with most of the upper Paleozoic rocks in Utah and adjacent areas until major thrusting associated with the Sevier orogeny disrupted the units (fig. 14).

To the south of the Tar Sand Triangle, the White Rim Sandstone is in hydrologic continuity with the De Chelly and Coconino Sandstones. In this region, an upper aquifer consisting of the White Rim, De Chelly, and Coconino Sandstones is separated from a lower aquifer consisting of the Cedar Mesa and Esplanade Sandstones by the Organ Rock and Hermit Shales that act as the confining units even where fractured (Geldon, in press). Thus, the upper and lower aquifers would be expected to be mostly independent hydrologically.

West of the Tar Sand Triangle and northwest of a line marking the pinchout of the Organ Rock and Hermit Shales, there is just one sandstone aquifer variously identified as the White Rim, Cedar Mesa, or Queantoweap. Farther to the west, these sandstones correlate with the Talisman Quartzite and the Arcturus Formation, which consist of dolomitic sandstone. Locally, some of these units are absent due to nondeposition or subsequent removal, but, if restored, the correlative units may have formed a continuous hydrologic pathway. Thus, it is possible that water and petroleum flowed easterly within Permian sandstone aquifers for more that 300 km from eastern Nevada to eastern Utah. After Sevier thrusting, the thrust faults probably fragmented the hydrologic system into separate systems. Ground water and petroleum may have migrated along the faults into permeable zones and thence eastward to the White Rim, or the thrust faults may have impeded flow.

Northwestward from the Tar Sand Triangle the White Rim Sandstone correlates with the Diamond Creek Sandstone. In the Oquirrh Basin of northwestern Utah, the Pennsylvanian-Permian Oquirrh Group forms a thick (4,300 m, 14,000 ft) section that includes abundant sandstone. In northeastern Utah the partly equivalent Middle Pennsylvanian to Lower Permian Weber Sandstone and Upper Mississippian to Lower Permian Wells Formation are important aquifers. Before Sevier thrusting, the Pennsylvanian-Permian sandstones (Oquirrh Group, part of Wells Formation, and Weber Sandstone) were probably in hydrologic communication with the overlying Diamond Creek Sandstone and

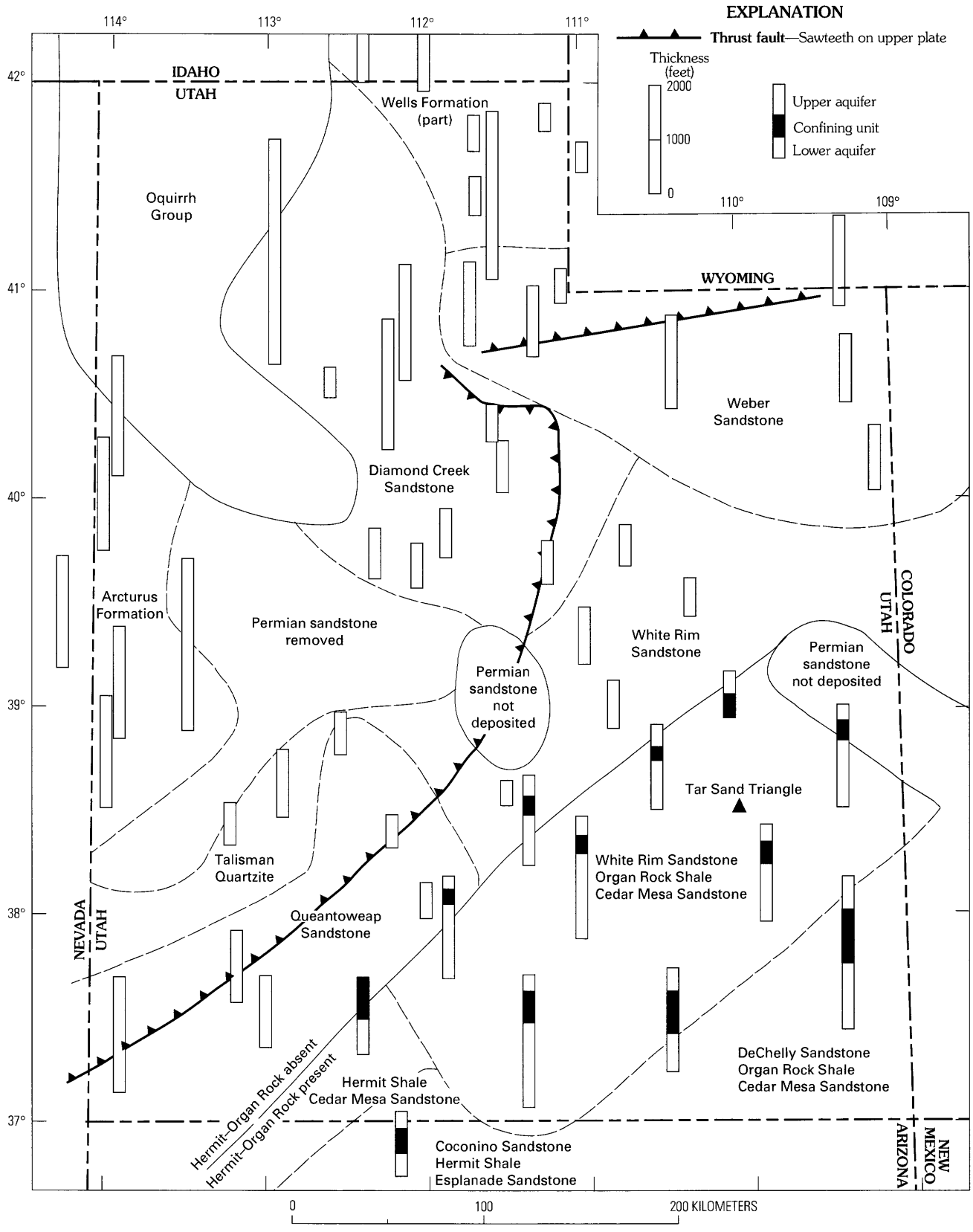

Figure 14. Pennsylvanian and Permian aquifers (dashed lines) in Utah and adjacent States. Height of bar is proportional to thickness. Aquifers are unshaded, and confining units are shaded. Triangle indicates location of Tar Sand Triangle. Compiled from numerous sources, principally Baars (1962), Blakey and others (1988), Hintze (1988), and Geldon (in press).

with the White Rim Sandstone. Thus, it may have been possible for ground water and petroleum to have flowed from northern Utah, southern Idaho, and southern Wyoming south to the Tar Sand Triangle. After thrusting, the Oquirrh Group and Diamond Creek Sandstone were separated from the Weber and White Rim by thrust faults that may have isolated the flow systems.

The White Rim and Cedar Mesa Sandstones both grade into undifferentiated Cutler Formation arkose to the east of the Tar Sand Triangle. Still farther to the east, the Culter thins to zero on the flanks of the Uncompahgre uplift. Long-range migration of ground water and oil from the east was virtually impossible, although ground-water flow from the Uncompahgre uplift to the Tar Sand Triangle was possible.

In summary, long-range transport of petroleum through Pennsylvanian and Permian sandstone aquifers that were hydrologically continuous with the White Rim Sandstone was possible until Sevier thrusting. The aquifers would have allowed long-range flow from the south, west, and north but not from the east. After thrusting, long-range migration would have been impeded or diverted by the thrust faults.

HYDROCARBON SOURCE ROCKS

Significant organic-rich potential source rocks are numerous in the region (fig. 15). As will be shown later, ground-water and maturation history rule out certain of these sources.

The Late Proterozoic Chuar Group and equivalents are present in the subsurface from north-central Arizona through central Utah to southwestern Wyoming (fig. 15) (Palacas, 1992). Where exposed in the Grand Canyon, the Chuar Group (divided into the Galeros Formation below and the Kwagunt Formation above) is 1,637 m (5,370 ft) thick and consists of predominantly very fine grained siliciclastic rocks and thin sequences of sandstone and stromatolitic and cryptalgal carbonate rocks (Reynolds and others, 1988). More than half of the sequence consists of organic-rich gray to black mudstone and siltstone. Environments of deposition include a sediment-starved basin rich in organic material, a coastal or alluvial plain, and a mixed coastal or paludal swamp and alluvial plain (Reynolds and others, 1988). Total organic carbon content may be as much as 10 weight percent (Chidsey and others, 1990), extractable organic matter as much as 4,000 ppm, and genetic potential ($S_1 + S_2$) as much as 16,000 ppm (average ~6,000 ppm) (Palacas and Reynolds, 1989). A 281-m (920 ft)-thick section consisting of the Walcott Member of the Kwagunt Formation (upper part) averages 3 weight percent total organic carbon (Palacas and Reynolds, 1989). Source rocks in the Walcott Member are within the oil generation window, whereas those in other units of the Chuar are mature to supermature. Saturated hydrocarbon gas chromatograms, biomarker distributions, and carbon isotope data suggest a common origin for solid bitumens in solution-collapse breccia pipes in northern Arizona and for bitumens ("tar") in the tar-sand deposits of southern Utah, including the Tar Sand Triangle (Wenrich and Palacas, 1990). The Chuar Group has been considered the source for heavy oil in the Tar Sand Triangle and elsewhere in the Colorado Plateau (Allin, 1990). Although Chuar Group samples are similar in some respects to breccia-pipe and tar-sand samples, the similarities are not striking enough to conclude with certainty that the Chuar Group was the source (Wenrich and Palacas, 1990). The Mississippian Chainman Shale is the major petroleum source rock in the Great Basin of Nevada and western Utah (fig. 15) (Poole and Claypool, 1984). The Chainman consists of flysch that accumulated in a trough in front of the Antler orogenic highlands. The Chainman contains from less than 0.1 to 10 weight percent total organic carbon, from 15 to 2,600 ppm bitumen, and from 10 to 2,000 ppm hydrocarbons (Poole and Claypool, 1984). Locally, it has the characteristics of a low-grade oil shale on the basis of Rock-Eval total hydrocarbon data (S_1+S_2) that suggest pyrolytic oil yields of 12–19 mg/g (3–5 gal/ton). Its organic matter is favorable for petroleum generation in many parts of east-central Nevada and west-central Utah, and the Chainman has been identified as the source rock for several oil fields in Nevada. Oil generation and migration probably occurred first in the late Paleozoic or Mesozoic, perhaps associated with the Sevier orogeny, and later during basin and range subsidence. Several other units in the Great Basin area are also potential source rocks, including the Ordovician Vinini Formation, the Upper Devonian and Lower Mississippian Pilot Shale, the Mississippian Delle Phosphatic Member of the Woodman Formation, and the Upper Mississippian to Middle Pennsylvanian Manning Canyon Shale.

Shales of the Upper Mississippian Doughnut Formation in northeastern Utah and northwestern Colorado are in part equivalent to the Chainman (Meissner and others, 1984). They represent lagoonal and estuarine deposits in a shallow trough. Total organic carbon content averages 2.5 weight percent. Although the maturation level of the Doughnut is favorable for oil generation, the quantity of hydrocarbons is not significant (Swetland and others, 1978).

The Middle and Upper Pennsylvanian Hermosa Group contains kerogen-rich black shale interbedded with evaporites and carbonate rocks mainly in the Paradox Formation of the Paradox Basin of southeastern Utah and southwestern Colorado. The black shales were the source of petroleum that now resides in overlying carbonate reservoir rocks (Hite and others, 1984). The shales contain as much as 21 weight percent total organic carbon. One 9-m (30 ft)-thick interval averaged 2.5 weight percent total organic carbon. The shales are thought to have produced 400 million barrels (53.6 million metric tons) of oil and 1 trillion cubic feet (28.4×10^9 m^3) of gas (Baars and Stevenson, 1982). Geothermal gradients suggest that maximum burial temperatures were as high as

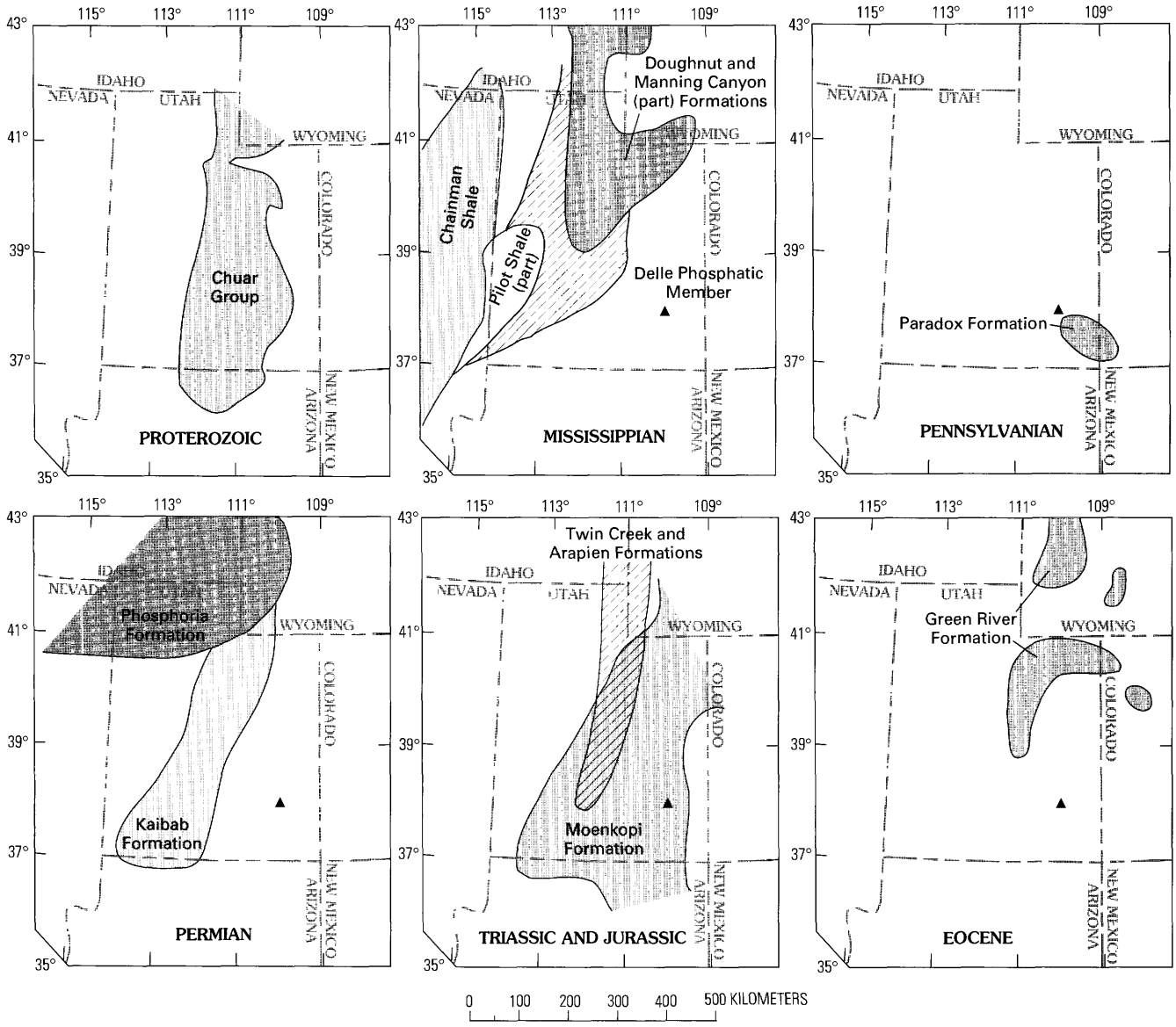

Figure 15. Potential source rocks in Utah and adjacent States for various time periods. Triangle indicates location of Tar Sand Triangle. Compiled from J.G. Palacas (written commun., 1992) and Meissner and others (1984).

77°C (170°F). Vitrinite reflectance and transformation ratios ($S_1/(S_1+S_2)$) are variable and difficult to interpret, but some of these values indicate conditions within the oil generation window (Hite and others, 1984). Analysis of burial history indicates that the Hermosa Group in the eastern and thickest part of the Paradox Basin was within the oil generation window in Permian and Triassic time (V.F. Nuccio, written commun., 1993).

The Lower Permian Phosphoria Formation of southeastern Idaho and adjacent States formed at the periphery of a foreland basin between the Paleozoic continental margin and the North American cratonic shelf (Maughan, 1984). It contains two members, the Meade Peak and Retort Phosphatic Shale, that consist of dark-gray shale, phosphorite, and chert of marine origin. The members represent the maximum marine transgression in two cycles. Total organic carbon content in the Meade Peak Member is typically 0.9–4.2 weight percent and hydrocarbon content 11–1,280 ppm (Claypool and others, 1978). In the Retort Phosphatic Shale Member, total organic carbon content ranges from 0.5 to 16 weight percent, and hydrocarbon content ranges from 10 to 3,320 ppm (Claypool and others, 1978). A total of 1.75×10^9 million tons of extractable heavy hydrocarbons has been calculated for the Phosphoria black shale (Claypool and others, 1978), most of which is in mature and overmature rocks. The Phosphoria is thought to be the source of much of the petroleum in upper Paleozoic rocks of the northern and central Rocky Mountain region (Claypool and others, 1978) and has been proposed as the source for the Tar Sand Triangle deposit (Demaison, 1977).

The Lower Permian Toroweap and Kaibab Formations consist of clastic rocks, limestone, and gypsum deposited on a stable continental shelf in central Utah (Bissell, 1969). Evidence of oil is present but sparse. The Kaibab is a reservoir for oil in the Upper Valley field on the Kaiparowits Plateau of southwestern Utah (Doelling, 1975). Asphalt fills vugs and other cavities, and sandstone and sandy limestone beds are petroliferous (Gilluly, 1929; Hunt and others, 1953; Smith and others, 1963). In the Kaiparowits Plateau, the Kaibab reached hydrocarbon maturity in the Late Cretaceous, and conditions remained favorable for oil generation through the Miocene (V.F. Nuccio, written commun., 1993). Because of its marine character, the Kaibab has been suggested as a possible source rock for the Tar Sand Triangle (Baars and Seager, 1970); however, abundant organic-rich black shales or other likely source rocks have not been documented. The oil that is present probably migrated in from another source.

The Lower and Middle(?) Triassic Moenkopi Formation is a redbed sequence that grades from dominantly fluvial clastic rocks in east Utah to shallow-marine limestone, dolomite, and siltstone in west Utah (Stewart and others, 1972). The Moenkopi is a reservoir for oil in the Virgin oil field in southwestern Utah. Petroliferous material has been reported in sandy siltstone and siltstone but was probably introduced after sedimentation (Stewart and others, 1972). Detrital asphalt has been reported from the Sinbad Limestone Member (Gilluly, 1929). Abundant organic-rich black shales have not been reported.

The Middle Jurassic Twin Creek and Arapien Formations of central Utah have been proposed as petroleum source rocks (Britt and Howard, 1982; Meissner and others, 1984). Surface samples have total organic carbon contents of 1.1 weight percent or less, but subsurface samples have total organic carbon contents as high as 4 weight percent.

Cretaceous shales are reported to have source rock potential, namely the Lower Cretaceous Skull Creek Shale and the Upper Cretaceous Mancos Shale (Britt and Howard, 1982), Mowry Shale, Greenhorn Limestone Member of the Mancos Shale, Niobrara Formation, and equivalents (Meissner and others, 1984). For the latter group of formations total organic carbon content ranges from 0.7 to 4.0 weight percent (Meissner and others, 1984). The organic material is dominantly type II kerogen (oil prone). In other Upper Cretaceous units, such as the Frontier, Mesaverde, and Lance, organic matter is dominantly type III kerogen (gas prone). Because Upper Cretaceous shales have not reached thermal maturity in adjacent areas, it is doubtful whether they did in the Canyonlands area.

The Paleocene and Eocene Green River Formation is an important petroleum source rock in the Uinta Basin of northern Utah (Fouch and others, 1992). The Green River Formation consists of lacustrine and fluvial sediments that accumulated in a closed basin. Almost 500 million barrels of oil, 12–13 billion barrels of tar, and more than 1.3 trillion cubic feet of gas were derived from the Green River through 1991 (Fouch and others, 1992, in press). Some kerogenous carbonate beds ("oil shale") have total organic carbon contents as high as 60 weight percent and averaging about 6.0 weight percent. Hydrogen indexes are as high as 500 mg hydrocarbons per gram of total organic carbon. The Green River is both source and reservoir rock. Oil generation probably began at the base of the Green River about 40 Ma and high in the section about 25 Ma (Fouch and others, in press).

DIAGENETIC EVIDENCE FOR HYDROCARBON MIGRATION

Pennsylvanian and Permian rocks of the Canyonlands area typically are red, and white rocks are distinctive. Field observations show that bleaching occurred after reddening. Bleaching clearly involves reduction, and probably also dissolution, of iron. Water-soluble organic acids are known to reduce and dissolve iron (McMahon and Chapelle, 1991; Cozzarelli and Baedecker, 1992). Organic-acid generation typically predates oil generation (Surdam and others, 1989). Organic acids can increase porosity by the dissolution of carbonate cement (Surdam and others, 1993). Assuming that bleaching is caused by water-soluble organic acids, the field distribution of bleached rock indicates the passage of organic-acid-bearing ground water (Surdam and others, 1993) and suggests sources for subsequently generated petroleum.

The coloration of Pennsylvanian and Permian rocks was examined from White Canyon northeast to the confluence of the Green and Colorado Rivers (fig. 16). The White Rim Sandstone is characteristically bleached in this entire area. The Cedar Mesa Sandstone is thoroughly bleached from White Canyon to Gypsum Canyon. At The Needles on the south side of the Colorado River and at The Maze on the north side of the river, the Cedar Mesa shows interfingering red and bleached layers. The color variation is not lithologically controlled because the Cedar Mesa is homogeneous sandstone; instead, the variation may be a weakening of the bleaching. Approximately 5 km northeast of the Green River, the Cedar Mesa begins to interfinger with red, undifferentiated Cutler Formation arkose. The transition from white to red rocks is likely the result of the oxidation of organic acids by hematite in the rocks.

Sandstones of the Pennsylvanian Hermosa Group and Permian Cutler Group exposed in Dark and Gypsum Canyons are mostly red, except for fracture-related bleaching (fig. 16). Bleaching has occurred along networks of fractures and in seemingly unfractured rock. Isolated spheroidal reduction spots also are present. In Gypsum Canyon a progression from thin (1 mm) reduction zones at the edges of isolated fractures to thick (20 cm) reduction zones mantling networks of fractures to thoroughly bleached rock showing

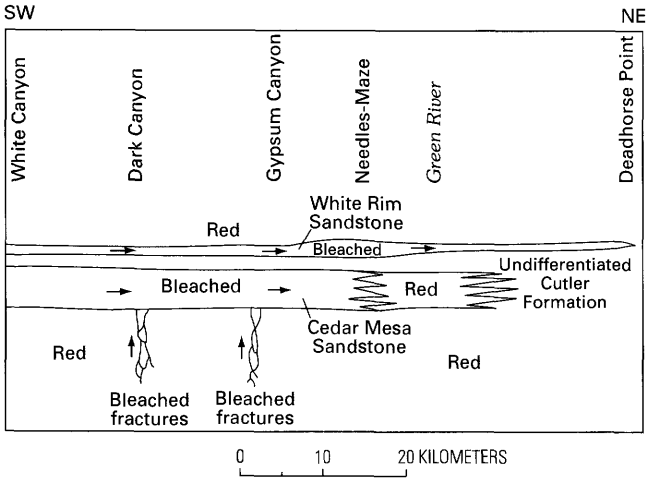

Figure 16. Schematic diagram showing distribution of red and bleached (white) Permian rocks in the Canyonlands area and inferred flow directions (arrows) of organic-acid-bearing ground water.

no sign of original red color is present. The progression shows that the bleaching postdated the reddening and that most bleaching is related to fractures.

Inferred ground-water flow directions are upward and northeastward. Because hydrocarbon generation occurs first at depth and because basin ground-water flow is typically upward, it is reasonable to assume upward flow in the fracture systems of the Hermosa and Cutler (fig. 16). In the Cedar Mesa Sandstone, the transition from white to red suggests northeastward transport of organic acids. Likewise, the pinchout of the White Rim Sandstone into red Cutler arkoses suggests northeastward ground-water flow. Thus, the coloration of rocks suggests that the source for petroleum in the Tar Sand Triangle was to the southwest and was stratigraphically below the White Rim Sandstone.

Other diagenetic reactions help constrain the timing of oil migration (Hansley, 1992, unpublished data). Nonferroan calcite cement and possibly gypsum precipitated soon after sedimentation, and later this calcite dissolved. An inverse relationship between calcite and oil suggests that organic acids preceding the oil caused the calcite dissolution. Abundant quartz overgrowths protrude into secondary voids and are coated by oil. Silica may have been transported by organo-silica complexes. Kaolinite fills pores and is oil stained (P.L. Hansley, unpublished data). Pyrite was oxidized after oil emplacement (Hansley, 1992). These data suggest that oil migration took place late in the burial history, possibly in the Late Cretaceous or early Tertiary.

A minimum age is indicated by the relationship between oil and Grand Canyon downcutting by the Colorado River. Oil is present on both sides of the canyon of the Green River, a tributary of the Colorado (J.E. Huntoon, oral commun. to P.L. Hansley, 1992). Therefore, oil must have been emplaced prior to canyon downcutting (P.L. Hansley, unpublished data). Thus, an age of about 10 Ma for initiation of Grand Canyon downcutting (Lucchitta, 1972; Larson and others, 1975) is a minimum age for oil emplacement.

EVALUATION OF HYDROCARBON SOURCES

A favorable petroleum source rock must be consistent with ground-water flow directions and with the quantity of organic matter and maturity of the source rock. Each potential petroleum source requires a particular flow direction to the reservoir; however, the implied flow direction may not be consistent with actual flow directions. Flow history thus can be used to evaluate the likelihood of a particular source. The Tar Sand Triangle is estimated to contain 16 billion barrels of tar (Campbell and Ritzma, 1979). The source must have the potential of yielding such a large quantity. The presence of adequate volumes of thermally mature organic-rich rocks is considered the most critical factor that limits the ultimate hydrocarbon reserves (Demaison, 1977). Both the amount of hydrocarbons and their maturity must be favorable. Further, the source must be mature during the time that ground-water flow is favorable for transport.

Petroleum from the Chuar Group must have flowed mainly east to reach the Tar Sand Triangle, although the wide distribution of the Chuar permitted flow that was southeast, northeast, and directly upward (fig. 15). Petroleum migration would have been crossformational up to the Permian aquifers, presumably through faults and fractures. From there, flow along the Permian aquifers, such as the White Rim, Cedar Mesa, and equivalents, would have been easy. Flow directions were favorable during the Late Jurassic to middle late Cenomanian and the late Campanian. The thickness and organic content of the organic-rich zones (Palacas and Reynolds, 1989) suggest that enough petroleum could have been generated to account for that in the Tar Sand Triangle. The fact that some of the Chuar is overmature (Palacas and Reynolds, 1989) suggest that some petroleum may have been generated prior to maximum burial, possibly in the Late Jurassic or in the Early to mid-Cretaceous. A northeast flow direction is also consistent with bleaching discussed above. From the standpoint of ground-water flow and quantity and maturity of organic matter, the Chuar is a highly plausible source rock.

The Chainman Shale and other potential source rocks, such as the Vinini Formation, Pilot Shale, Delle Phosphatic Member of the Woodman Formation, and the Manning Canyon Shale, in Nevada and western Utah all require eastward or northeastward ground-water flow directions. Such flow occurred from Late Jurassic to middle late Cenomanian and late Campanian. Favorable Permian aquifers include the

Arcturus Formation, Talisman Quartzite (prior to metamorphism), Queantoweap Sandstone, and White Rim Sandstone. The presumed late Paleozoic–Mesozoic age of oil generation (Poole and Claypool, 1984) is compatible with Late Jurassic to late Campanian migration. The greatest difficulty with this source is the migration across the zone of thrust faults in central and western Utah. Perhaps oil migration occurred early in the orogenic episode, before the faults had propagated eastward. Alternatively, oil migrated across and along the thrusts. The Chainman and other formations in Nevada and western Utah are thus plausible sources for oil in the Tar Sand Triangle; however, there are major difficulties with this interpretation.

The Doughnut Formation, a partial equivalent to the Chainman, requires a southeastward ground-water flow direction to reach the Tar Sand Triangle. There was no known time during which ground-water flow was southeastward except in the last 10 m.y., and the dissection of the tar by the Green River rules out an age this young, as discussed previously. Thus, the Doughnut is an unlikely source.

A source in the Paradox Formation requires petroleum to migrate westward or northwestward. Ground water flowed northwest during the lengthy period from Late Permian to Middle Jurassic and flowed northward from the middle late Campanian to the late Miocene. The quantity of contained organic matter (Baars and Stevenson, 1982; Hite and others, 1984) suggests that the Paradox could account for the tar in the Tar Sand Triangle. Calculations suggest that organic matter in the Paradox Formation 30 km east of the Tar Sand Triangle reached maturity in the Late Permian to Early Triassic (V.F. Nuccio, written commun., 1993). These facts are consistent with oil generation and northeast migration to the Tar Sand Triangle in the Late Permian to Middle Jurassic period. The middle late Campanian to late Miocene is another possible time of migration from the Paradox to the Tar Sand Triangle. To reach the White Rim Sandstone in the Tar Sand Triangle, petroleum from the Paradox must have migrated through the undifferentiated Permian Cutler Formation, the Cedar Mesa Sandstone, and the Organ Rock Shale. Although the Cedar Mesa and White Rim are thoroughly bleached, suggestive of alteration by organic acids, the undifferentiated Cutler typically is red, which suggests a scarcity of organic acids (fig. 16). The Organ Rock has low permeability and also typically is red. The White Rim pinches out to the southeast and therefore would be favorable as a facies trap for southeast-migrating petroleum but not for northwest-migrating petroleum. Thus, favorable times for petroleum migration from the Paradox to the White Rim were the Late Permian to Middle Jurassic and the middle late Campanian to late Miocene; however, the configuration of aquifers and the distribution of alteration fails to confirm such migration.

The Phosphoria Formation requires southeastward petroleum migration. As discussed for the Doughnut, there was no time characterized by such flow prior to Grand Canyon downcutting. Thrust faults also would have isolated the flow in northwestern Utah from that in southeastern Utah. Despite the abundant mature hydrocarbons in the Phosphoria (Claypool and others, 1978), it is an unlikely source owing to the unfavorable migration direction.

The Kaibab and Toroweap Formations, possibly partly correlative with the Phosphoria Formation, require ground-water flow to the east or northeast. Favorable flow existed from the Late Jurassic to the middle late Cenomanian and during the late Campanian. Because the White Rim is probably facies equivalent to the Toroweap and possibly to the lower Kaibab (Baars, 1979), a hydraulic connection to the Tar Sand Triangle is very straightforward. A serious drawback to a Kaibab or Toroweap source is the lack of suitable source beds. The contained petroleum mainly fills vugs and other cavities (Gilluly, 1929; Hunt and others, 1953; Smith and others, 1963), and thus probably is mostly secondary. Maturity calculations suggest that rocks in the Kaiparowits area reached the petroleum generation window in the Late Cretaceous (Vito Nuccio, written commun., 1993). Despite the convenient hydrologic pathway, favorable flow directions, and maturity, these units cannot be considered viable source rocks because of the lack of thick organic-rich source beds.

The Moenkopi is stratigraphically above the White Rim Sandstone of the Tar Sand Triangle. Most of the Moenkopi extends to the west of the Tar Sand Triangle. Petroleum would have had to migrate downward and eastward. Although the Moenkopi is in hydrologic continuity with the White Rim, downward migration of petroleum is problematic. The Moenkopi is a confining unit (Geldon, in press), and thus downward flow would be impeded. Source beds are present but not abundant. The lack of abundant organic-rich source beds also is unfavorable for a Moenkopi source.

The Twin Creek and Arapien Formations are in the thrust belt of western Utah. If they were sources, petroleum would have migrated downward stratigraphically, eastward and across the thrust faults. Eastward flow was most likely during the late Campanian. Downward flow would have been through two confining units, the Upper Triassic Chinle Formation and the Lower and Middle(?) Triassic Moenkopi Formation, and the thrust faults would have been an additional hydrologic barrier. Organic matter is abundant in certain samples, but whether the total quantity is sufficient to account for the Tar Sand Triangle is questionable. Thrusting may have repeated units enough to bury the Twin Creek and Arapien to maturation depths. Thus, the hydrologic barriers and the dubious quantity of hydrocarbons indicate that the Twin Creek and Arapien Formations are unlikely source rocks for the Tar Sand Triangle.

The Mancos and other Upper Cretaceous shales require downward migration of petroleum through many confining units including the Brushy Basin Member of the Morrison Formation, the Chinle Formation, and the Moenkopi Formation. The buoyancy of oil and the low permeability of these

confining units argues against such migration. The generally red rocks above the White Rim provide no evidence of the migration of organic matter.

The Green River Formation requires flow that was southward and stratigraphically downward. Southward flow is unknown prior to Grand Canyon downcutting. Downward flow would have had to traverse several confining units including the Mancos Shale, the Brushy Basin Member of the Morrison Formation, the Chinle Formation, and the Moenkopi Formation. Although the Green River has sufficient hydrocarbon content and maturity, it is unlikely, because of buoyancy, the presence of confining units, and an unfavorable flow direction, that petroleum could have reached the Tar Sand Triangle.

SUMMARY AND CONCLUSIONS

Six distinctive periods of ground-water flow are recognized in the Tar Sand Triangle of southeastern Utah. (1) From Late Permian to Middle Jurassic (256–157 Ma), ground water flowed northwest with tributary flow southwest off the Uncompahgre uplift. (2) From the Late Jurassic to the middle to late Cenomanian (155–93.5 Ma), ground water flowed northeast from the Elko and Sevier highlands. (3) From the late Cenomanian to the Campanian (93.5–76.6), the Mancos Shale was deposited and conditions were almost hydrostatic. (4) During the late Campanian (79.4–74 Ma), ground water flowed eastward from the Sevier highlands. (5) From middle late Campanian to late Miocene (74–10 Ma), flow was northward toward the Uinta Basin. (6) From late Miocene (10 Ma) to the present, flow was generally southwestward, but dissection by the Colorado River set up highly localized flows.

Analysis of the transmissivity of the hydrostratigraphic units through time shows that flow was mostly parallel with bedding in the Lower Permian White Rim Sandstone of the Tar Sand Triangle. There are no detectable transmissivity variations that would cause significant upward or downward flow.

Regional Pennsylvanian and Permian aquifers are widely distributed in Utah and adjacent States, and many are hydrologically connected. Thrust faults typically form barriers to flow and may have divided the hydrologic systems of western and eastern Utah. Thus, ground-water flow probably was mostly unimpeded until the Sevier orogeny. After the Sevier orogeny, hydrologic systems probably were more localized except where ground water found favorable routes across the thrust faults.

Potential source rocks for the hydrocarbon in the White Rim Sandstone include the (1) Late Proterozoic Chuar Group in central Utah, (2) Mississippian Chainman Shale and other rocks in Nevada and western Utah, (3) Upper Mississippian Doughnut Formation in northeastern Utah and northwestern Colorado, (4) Middle Pennsylvanian Paradox Formation in the Paradox Basin of Utah and Colorado, (5) Lower Permian Phosphoria Formation of southeastern Idaho and adjacent States, (6) Lower Permian Toroweap and Kaibab Formations in central Utah, (7) Lower and Middle(?) Triassic Moenkopi Formation in Utah, (8) Middle Jurassic Twin Creek and Arapien Formations in central Utah, (9) Lower Cretaceous Skull Creek Shale, Upper Cretaceous Mancos Shale, Mowry Shale, Greenhorn Limestone Member of the Mancos Shale, Niobrara Formation, and equivalents, and (10) Paleocene and Eocene Green River Formation in the Uinta Basin of northern Utah.

Source rocks that require southward migration are least likely because southward ground-water flow is unknown. Thus, despite the richness in hydrocarbons, the Doughnut, Phosphoria, and Green River Formations are unlikely sources for hydrologic reasons.

Paradox Formation source rocks, which require northward or northwestward migration, were hydrologically favored during two periods, the Late Permian to Middle Jurassic and the middle late Campanian to late Miocene. Both periods may have been within the oil generation window. The main difficulties with a Paradox source are (1) ground water would have had to pass through the undifferentiated Cutler Formation which shows no evidence of large amounts of organic acids or oil, and (2) the pinchout of the White Rim Sandstone is favorable for trapping oil from the northwest not from the southeast.

The Chainman Shale and related units in Nevada, as well as units in western Utah such as the Twin Creek and Arapien Formations, require long-distance eastward migration across the thrust belt. The direction of ground-water flow was favorable from the Late Jurassic to the middle late Cenomanian and during the late Campanian. Many of these units, notably the Chainman Shale, may have contained sufficient organic matter to supply the Tar Sand Triangle. The major drawback is the migration across the thrust belt; however, migration could have occurred prior to thrusting.

Potential source rocks west of the Tar Sand Triangle but east of the thrust belt, namely the Chuar Group and the Toroweap, Kaibab, and Moenkopi Formations, are very favorable from a hydrologic standpoint. The direction of ground-water flow was favorable from the Late Jurassic to the middle late Cenomanian and during the late Campanian. Lateral flow would have been easy through the Queantoweap, Esplanade, Cedar Mesa, Coconino, and White Rim Sandstones. The direction of transport is consistent with field observations of bleaching of Pennsylvanian and Permian redbeds. The Toroweap, Kaibab, and Moenkopi are poor sources because of the scarcity of hydrocarbon-generating organic matter, but the Chuar Group contains abundant organic matter of sufficient maturity. Thus, given the present state of knowledge, the Chainman Shale (and other nearby units) and Paradox Formation cannot be ruled out, but the Chuar Group is the most likely source. In order to confirm that the Chuar or any other rock unit is indeed the source of

the Tar Sand Triangle heavy oils, the composition of the indigenous organic matter of the potential source rock must be determined and compared with that of tar sand oils. In other words, crude oil–source rock correlations made using, for example, biomarker and saturated and aromatic hydrocarbon distributions and carbon isotope ratios should be conducted in order to validate or to disqualify suspected source rocks.

REFERENCES CITED

Allin, D.L., 1990, Colorado Plateau subsurface water flow key: Oil and Gas Journal, v. 88, p. 52–54.

Baars, D.L., 1962, Permian System of Colorado Plateau: American Association of Petroleum Geologists Bulletin, v. 46, p. 149–218.

———1979, The Permian System: Four Corners Geological Society Field Conference, 9th, p. 1–6.

Baars, D.L., and Molenaar, C.M., 1971, Geology of Canyonlands and Cataract Canyon: Four Corners Geological Society Field Conference, 6th, Durango, Colo., 99 p.

Baars, D.L., and Seager, W.R., 1970, Stratigraphic control of petroleum in White Rim Sandstone (Permian) in and near Canyonlands National Park, Utah: American Association of Petroleum Geologists Bulletin, v. 54, p. 709–718.

Baars, D.L., and Stevenson, G.M., 1982, Subtle stratigraphic traps in Paleozoic rocks of the Paradox Basin, *in* Halbauty, M.T., ed., Deliberate search for the subtle trap: American Association of Petroleum Geologists Memoir 32, p. 131–158.

Bissell, H.J., 1969, Permian and Lower Triassic transition from the shelf to basin (Grand Canyon, Arizona to Spring Mountains, Nevada): Four Corners Geological Society Field Conference, 5th, Guidebook, p. 135–169.

Blakey, R.C., 1974, Stratigraphic and depositional analysis of the Moenkopi Formation, southeastern Utah: Utah Geological and Mineralogical Survey Bulletin, v. 104, 81 p.

Blakey, R.C., Basham, E.L., and Cook, M.J., 1993, Early and Middle Triassic paleogeography, Colorado Plateau and vicinity, *in* Morales, M., ed., Aspects of Mesozoic geology and paleontology of the Colorado Plateau: Museum of Northern Arizona Bulletin 59, p. 13–26.

Blakey, R.C., and Gubitosa, Richard, 1983, Late Triassic paleogeography and depositional history of the Chinle Formation, southern Utah and northern Arizona, *in* Reynolds, M.W., and Dolly, E.D., eds., Mesozoic paleogeography of the West-Central United States: Rocky Mountain Section, Society of Economic Paleontologists and Mineralogists, Rocky Mountain Paleogeography Symposium, v. 2, p. 57–77.

Blakey, R.C., Peterson, Fred, and Kocurek, Gary, 1988, Synthesis of late Paleozoic and Mesozoic eolian deposits of the Western Interior of the United States: Sedimentary Geology, v. 56, p. 3–125.

Britt, T.L., and Howard, E.L., 1982, Oil and gas potential of the central Utah hingeline-thrust belt region, *in* Powers, R.B., ed., Geologic studies of the Cordilleran thrust belt: Rocky Mountain Association of Geologists, v. 2, p. 475–505.

Campbell, J.A., and Ritzma, H.R., 1979, Geology and petroleum resources of the major oil-impregnated sandstone deposits of Utah: Utah Geological and Mineral Survey Special Studies 50, 24 p.

Chan, M.A., 1989, Erg margin of the Permian White Rim Sandstone, SE Utah: Sedimentology, v. 36, p. 235–251.

Chan, M.A., and Kocurek, Gary, 1988, Complexities in eolian and marine interactions—Processes and eustatic controls on erg development: Sedimentary Geology, v. 56, p. 283–300.

Chidsey, T.C., Allison, M.L., and Palacas, J.G., 1990, Potential for Precambrian source rock in Utah: American Association of Petroleum Geologists Bulletin, v. 74, p. 1319.

Claypool, G.E., Love, A.H., and Maughan, E.K., 1978, Organic geochemistry, incipient metamorphism, and oil generation in black shale members of Phosphoria Formation, Western Interior United States: American Association of Petroleum Geologists Bulletin, v. 62, p. 98–120.

Clemmensen, L.B., Olsen, Henrik, and Blakey, R.C., 1989, Erg-margin deposits in the Lower Jurassic Moenave Formation and Wingate Sandstone, southern Utah: Geological Society of America Bulletin, v. 101, p. 759–773.

Cobban, W.A., and Hook, S.C., 1989, Mid-Cretaceous molluscan record from west-central New Mexico: New Mexico Geological Society Annual Field Conference, 40th, Guidebook, p. 247–264.

Cozzarelli, I.M., and Baedecker, M.J., 1992, Oxidation of hydrocarbons coupled to reduction of inorganic species in groundwater, *in* Kharaka, Y.K., and Maest, A.S., Water-rock interaction: Rotterdam, A.A. Balkema, p. 275–278.

Craig, L.C., 1981, Lower Cretaceous rocks, southwestern Colorado and southeastern Utah: Rocky Mountain Association of Geologists Field Conference, 1981, p. 195–200.

Craig, L.C., Holmes, C.N., Cadigan, R.A., Freeman, V.L., Mullens, T.E., and Weir, G.W., 1955, Stratigraphy of the Morrison and related formations, Colorado Plateau Region, a preliminary report: U.S. Geological Survey Bulletin 1009–E, p. 125–168.

Demaison, G.J., 1977, Tar sands and supergiant oil fields: American Association of Petroleum Geologists Bulletin, v. 61, p. 1950–1961.

Doelling, H.H., 1975, Geology and mineral resources of Garfield County, Utah: Utah Geological and Mineralogical Survey Bulletin 107, 175 p.

Dubiel, R.F., 1989, Depositional and climatic setting of the Upper Triassic Chinle Formation, Colorado Plateau, *in* Lucas, S.G., and Hunt, A.P., eds., Dawn of the age of dinosaurs in the American Southwest: Albuquerque, New Mexico Museum of Natural History, p. 171–187.

———1994, Triassic deposystems, paleogeography, and paleoclimate of the Western Interior, *in* Caputo, M.V., Peterson, J.A., and Franczyk, K.J., eds., Mesozoic Systems of the Rocky Mountain Region, USA: Denver, Rocky Mountain Section SEPM (Society for Sedimentary Geology), p. 133–168.

Dubiel, R.F., Parrish, J.T., Parrish, J.M., and Good, S.C., 1991, The Pangean megamonsoon—Evidence from the Upper Triassic Chinle Formation, Colorado Plateau: Palaios, v. 6, p. 347–370.

Fouch, T.D., Lawton, T.F., Nichols, D.J., Cashion, W.B., and Cobban, W.A., 1983, Patterns and timing of synorogenic sedimentation in Upper Cretaceous rocks of central and northeast Utah, *in* Reynolds, M.W., and Dolly, E.D., eds., Mesozoic paleogeography of the West-Central United States: Rocky Mountain Section, Society of Economic Paleontologists and Mineralogists,

Rocky Mountain Paleogeography Symposium, v. 2, p. 305–336.

Fouch, T.D., Nuccio, V.F., Anders, D.E., Rice, D.D., Pitman, J.K., and Mast, R.F., in press, The Green River petroleum system, Uinta Basin, Utah, USA, *in* Magoon, L.B., and Dow, W.G., eds., The petroleum system—From source to trap: American Association of Petroleum Geologists Memoir, 47 p.

Fouch, T.D., Nuccio, V.F., Osmond, J.C., MacMillan, Logan, Cashion, W.B., and Wandrey, C.J., 1992, Oil and gas in uppermost Cretaceous and Tertiary rock, Uinta Basin, Utah: Utah Geological Society Guidebook 20, p. 9–48.

Franczyk, K.J., Fouch, T.D., Johnson, R.C., Molenaar, C.M., and Cobban, W.A., 1992, Cretaceous and Tertiary paleogeographic reconstructions for the Uinta-Piceance basin study area, Colorado and Utah: U.S. Geological Survey Bulletin 1787–Q, 37 p.

Franczyk, K.J., Pitman, J.K., and Nichols, D.J., 1990, Sedimentology, mineralogy, palynology, depositional history of some uppermost Cretaceous and lowermost Tertiary rocks along the Utah Book and Roan Cliffs east of Green River: U.S. Geological Survey Bulletin 1787–N, 27 p.

Freethey, G.W., and Cordy, G.E., 1991, Geohydrology of Mesozoic rocks in the Upper Colorado River Basin in Arizona, Colorado, New Mexico, Utah, and Wyoming, excluding the San Juan Basin: U.S. Geological Survey Professional Paper 1411–C, 118 p.

Garven, Grant, Ge, S., Person, M.A., and Sverjensky, D.A., 1993, Genesis of stratabound ore deposits in the midcontinent basins of North America—1, The role of regional groundwater flow: American Journal of Science, v. 293, p. 497–568.

Geldon, A.L., in press, Hydrologic properties and flow systems of the Paleozoic rocks in the Upper Colorado River Basin, excluding the San Juan Basin, in Arizona, Colorado, Utah, and Wyoming: U.S. Geological Survey Professional Paper 1411–B, 411 p.

Gill, J.R., and Hail, W.J., Jr., 1975, Stratigraphic sections across Upper Cretaceous Mancos Shale–Mesaverde Group boundary, eastern Utah and western Colorado: U.S. Geological Survey Oil and Gas Investigations Chart OC–68.

Gilluly, James, 1929, Geology and oil and gas prospects of part of the San Rafael Swell, Utah: U.S. Geological Survey Bulletin 806–C, p. 69–130.

Hansen, W.R., ed., 1991, Suggestions to authors of the reports of the United States Geological Survey (7th ed.): Washington, D.C., U.S. Government Printing Office, 289 p.

Hansley, P.L., 1992, Diagenetic history of the Permian White Rim Sandstone Member, Cutler Formation, Tar Sand Triangle, Paradox Basin, Utah [abs.]: American Association of Petroleum Geologists Annual Convention, 1992, Official Program, p. 51.

Harland, W.B., Armstong, R.L., Cox, A.V., Craig, L.E., and Smith, D.G., 1990, A geologic time scale 1989: Cambridge, Cambridge University Press, 166 p.

Hintze, L.F., 1988, Geologic history of Utah: Brigham Young University Geology Studies Special Publication 7, 202 p.

Hite, R.J., Anders, D.E., and Ging, T.G., 1984, Organic-rich source rocks of Pennsylvanian age in the Paradox Basin of Utah and Colorado, *in* Woodward, Jane, Meissner, F.F., and Clayton, J.L., eds., Hydrocarbon source rocks of the greater Rocky Mountain region: Denver, Rocky Mountain Association of Geologists, p. 255–274.

Hubbert, M.K., 1953, Entrapment of petroleum under hydrodynamic conditions: American Association of Petroleum Geologists Bulletin, v. 37, p. 1954–2026.

Hunt, C.B., Averitt, Paul, and Miller, R.L., 1953, Geology and geography of the Henry Mountains region, Utah: U.S. Geological Survey Professional Paper 228, 234 p.

Huntoon, J.E., 1992, The Permian-Triassic boundary in south-central Utah—Stratigraphic relations and origin: Society of Economic and Petroleum Mineralogists 1992 Theme Meeting, Mesozoic of the Western Interior, Abstracts, p. 34.

Huntoon, J.E., and Chan, M.A., 1987, Marine origin of paleotopographic relief on eolian White Rim Sandstone (Permian), Elaterite Basin, Utah: American Association of Petroleum Geologists Bulletin, v. 71, p. 1035–1045.

Imlay, R.W., 1980, Jurassic paleobiogeography of the conterminous United States in its continental setting: U.S. Geological Survey Professional Paper 1062, 134 p.

Jobin, D.A., 1962, Relation of the transmissive character of the sedimentary rocks of the Colorado Plateau to the distribution of uranium deposits: U.S. Geological Survey Bulletin 1124, 151 p.

Kowallis, B.J., Christiansen, E.H., and Deino, A.L., 1991, Correlation of altered volcanic ash beds in the Brushy Basin Member of the Morrison Formation, Colorado Plateau: Geological Society of America Abstracts with Programs, v. 23, p. A295.

Kowallis, B.J., and Heaton, J.S., 1987, Fission-track dating of bentonites and bentonitic mudstones from the Morrison Formation in central Utah: Geology, v. 15, p. 1138–1142.

Kreitler, C.W., 1989, Hydrogeology of sedimentary basins: Journal of Hydrology, v. 106, p. 29–53.

Larson, E.E., Bradley, W.C., and Ozima, Minoru, 1975, Development of the Colorado River system in northwestern Colorado during the late Cenozoic: Four Corners Geological Society Field Conference, 8th, Guidebook, p. 97–102.

Lucchitta, Ivo, 1972, Early history of the Colorado River in the Basin and Range Province: Geological Society of America Bulletin, v. 83, p. 1933–1948.

Maughan, E.K., 1984, Geologic setting and some geochemistry of petroleum source rocks in the Permian Phosphoria Formation, *in* Woodward, Jane, Meissner, F.F., and Clayton, J.L., eds., Hydrocarbon source rocks of the greater Rocky Mountain region: Denver, Rocky Mountain Association of Geologists, p. 281–294.

McMahon, P.B., and Chapelle, F.H., 1991, Microbial production of organic acids in aquitard sediments and its role in aquifer geochemistry: Nature, v. 349, p. 233–235.

Meissner, F.F., Woodward, Jane, and Clayton, J.L., 1984, Stratigraphic relationships and distribution of source rocks in the greater Rocky Mountain region, *in* Woodward, Jane, Meissner, F.F., and Clayton, J.L., eds., Hydrocarbon source rocks of the greater Rocky Mountain region: Denver, Rocky Mountain Association of Geologists, p. 1–34.

Molenaar, C.M., 1971, Mesozoic stratigraphy of Canyonlands National Park and adjacent areas, *in* Baars, D.L., and Molenaar, C.M., eds., Geology of Canyonlands and Cataract Canyon: Four Corners Geological Society Field Conference, 6th, p. 49–60.

Molenaar, C.M., and Baars, D.L., 1985, Field trip no. 7, Canyonlands National Park float trip, Utah: Rocky Mountain Section,

Society of Economic Paleontologists and Mineralogists, Midyear Meeting, Field Guide, 74 p.

Northrop, H.R., and Goldhaber, M.B., eds., 1990, Genesis of the tabular-type vanadium-uranium deposits of the Henry basin: Economic Geology, v. 85, p. 215–269.

Obradovich, J.D., 1993, A Cretaceous time scale, *in* Caldwell, W.G.E., and Kauffman, E.G., eds., Evolution of the Western Interior basin: Geological Association of Canada Special Paper 39, p. 379–396.

Ochs, Steffen, and Chan, M.A., 1990, Petrology, sedimentology and stratigraphic implications of Black Dragon Member of the Triassic Moenkopi Formation, San Rafael Swell, Utah: The Mountain Geologist, v. 27, p. 1–18.

Padian, K., 1989, Presence of dinosaur Scelidosaurus indicates Jurassic age for the Kayenta Formation (Glen Canyon Group, northern Arizona): Geology, v. 17, p. 438–441.

Palacas, J.G., 1992, Appendix 5—Source-rock potential of Precambrian rocks in selected basins of the U.S., *in* Dyman, T.S., ed., Geologic controls and resource potential of natural gas in deep sedimentary basins in the United States: Final Report for Gas Research Institute, Contract 5090–260–2040, p. 161–167.

Palacas, J.G., and Reynolds, M.W., 1989, Preliminary petroleum source rock assessment of Upper Proterozoic Chuar Group, Grand Canyon, Arizona [abs.]: American Association of Petroleum Geologists Bulletin, v. 73, p. 397.

Peterson, Fred, 1988, A synthesis of the Jurassic system in the southern Rocky Mountain region, *in* Sloss, L.L., ed., The geology of North America, v. D–2, Sedimentary cover—North American craton: U.S.: Boulder, Colorado, Geological Society of America, p. 65–76.

———1994, Sand dunes, sabkhas, streams, and shallow seas—Jurassic paleogeography in the southern part of the Western Interior basin, *in* Caputo, M.V., Peterson, J.A., and Franczyk, K.J., eds., Mesozoic Systems of the Rocky Mountain Region, USA: Denver, Rocky Mountain Section SEPM (Society for Sedimentary Geology), p. 233–272.

Poole, F.G., and Claypool, G.E., 1984, Petroleum source-rock potential and crude-oil correlation in the Great Basin, *in* Woodward, Jane, Meissner, F.F., and Clayton, J.L., eds., Hydrocarbon source rocks of the greater Rocky Mountain region: Denver, Rocky Mountain Association of Geologists, p. 179–207.

Reynolds, M.W., Palacas, J.G., and Elston, D.P., 1988, Potential petroleum source rocks in the Late Proterozoic Chuar Group, Grand Canyon: U.S. Geological Survey Circular 1025, p. 49–50.

Sanford, R.F., 1990, Hydrogeology of an ancient arid closed basin—Implications for tabular sandstone-hosted uranium deposits: Geology, v. 18, p. 1099–1102.

———1992, A new model for tabular-type uranium deposits: Economic Geology, v. 87, p. 2041–2055.

Smith, J.F., Huff, L.C., Hinrichs, E.N., and Luedke, R.G., 1963, Geology of the Capitol Reef area, Wayne and Garfield Counties, Utah: U.S. Geological Survey Professional Paper 363, 302 p.

Steele, B.A., 1987, Depositional environments of the White Rim Sandstone member of the Permian Cutler Formation, Canyonlands National Park, Utah: U.S. Geological Survey Bulletin 1592, 20 p.

Stewart, J.H., Poole, F.G., and Wilson, R.F., 1972, Stratigraphy and origin of the Triassic Moenkopi Formation and related strata in the Colorado Plateau region: U.S. Geological Survey Professional Paper 691, 195 p.

Surdam, R.C., Crossey, L.J., Hagen, E.S., and Heasler, H.P., 1989, Organic-inorganic interaction and sandstone diagenesis: American Association of Petroleum Geologists Bulletin, v. 73, p. 1–23.

Surdam, R.C., Jiao, Z.S., and MacGowan, D.B., 1993, Redox reactions involving hydrocarbons and mineral oxidants—A mechanism for significant porosity enhancement in sandstones: American Association of Petroleum Geologists Bulletin, v. 77, p. 1509–1518.

Swetland, P.J., Clayton, J.L., and Sable, E.G., 1978, Petroleum source-bed potential of Mississippian-Pennsylvanian rocks in parts of Montana, Idaho, Utah, and Colorado: The Mountain Geologist, v. 15, p. 79–87.

Thorman, C.H., Ketner, K.B., Brooks, W.E., Snee, L.W., and Zimmermann, R.A., 1991, Late Mesozoic–Cenozoic tectonics in northeastern Nevada, *in* Raines, G.L., Lisle, R.E., Schafer, R.W., and Wilkinson, W.H., eds., Geology and ore deposits of the Great Basin: Reno, Geological Society of Nevada, p. 25–45.

Tubbs, R.E., Jr., 1989, Depositional history of the White Rim Sandstone, Wayne and Garfield Counties, Utah: The Mountain Geologist, v. 26, p. 101–112.

Turner, C.E., and Fishman, N.S., 1991, Jurassic Lake T'oo'dichi'—A large alkaline, saline lake, Morrison Formation, eastern Colorado Plateau: Geological Society of America Bulletin, v. 103, p. 538–558.

Tyler, Noel, and Ethridge, F.G., 1983, Depositional setting of the Salt Wash Member of the Morrison Formation, southwest Colorado: Journal of Sedimentary Petrology, v. 53, p. 67–82.

Wenrich, K.J., and Palacas, J.G., 1990, Organic matter and uranium in solution-collapse breccia pipes of northern Arizona and San Rafael Swell, Utah: U.S. Geological Survey Circular 1069, p. 36–50.

Willis, G.C., and Kowallis, B.J., 1988, Newly recognized Cedar Mountain Formation in Salina Canyon, Sevier County, Utah: Brigham Young University Geology Studies, v. 35, p. 57–61.

Wing, S.L., Bown, T.M., and Obradovich, J.D., 1991, Early Eocene biotic and climatic change in interior western North America: Geology, v. 19, p. 1189–1192.

Published in the Central Region, Denver, Colorado
Manuscript approved for publication April 6, 1995
Edited by Judith Stoeser
Graphics and photocomposition by Patricia L. Wilber

☆ U.S. GOVERNMENT PRINTING OFFICE: 1995 - 673-046 / 20000 REGION NO. 8